HELSINKI UNIVERSITY OF TECHNOLOGY
Department of Electrical and Communications Engineering

Jarno Tanskanen

Multiuser CDMA Power Control Simulator — Effects of Simple Prediction

This Licentiate Thesis has been submitted for official examination for the degree of Licentiate of Technology in Espoo, Finland.

Supervisor of the Thesis Iiro Hartimo

HELSINKI UNIVERSITY OF TECHNOLOGY

ABSTRACT OF THE LICENTIATE THESIS

Author: Jarno Tanskanen

Name of the Thesis: **Multiuser CDMA Power Control Simulator — Effects of Simple Prediction**

Date: Jan. 19, 1998 Number of pages: 50 + 28

Faculty: Electrical and Communications Engineering
Professorship: S-88, Signal Processing and Computer Technology

Supervisor: Professor Iiro Hartimo

In this work, reported in *the Publications*, predictivity of Rayleigh fading signals is investigated, and multiuser CDMA communications simulators are developed for uplink closed loop power control studies. With the simulator, effects of applying predictive filtering within the closed power control loop are studied. In the simulator, the prediction is applied to radio channel power responses which are modeled by Rayleigh fading signals.

Motivation of the work arises from the power control needs of CDMA systems. The system user capacity greatly depends on the power control system operation quality. In this work, power control system aims to maintain the received power levels of all the mobile users at an equal and constant level at the base station receiver which is one of the possible basis for the practical power control. As the closed power control loop naturally includes signal processing and radio propagation delays, an intuitive approach for achieving power control system improvements is to apply predictive filtering. The user capacities are not directly observed but the results are given in the form of bit-error-rate improvements, and as reductions in the mobile transmitter power consumption and received power level variance, the latter of which is now the actual control variable.

The simulator consists of fairly simple mobile transmitter, radio channel, base station receiver, and power controller models, and is implemented in COSSAP (Communications Simulation and System Analysis Program) environment. For predictive closed power control loop simulations, a single user, 5 user, and 10 user simulators are constructed along with a simulator employing an AWGN multiuser interference model. Naturally, also a non-predictive reference controller is used in the same simulators. Predictive filtering is performed by application of Heinonen-Neuvo polynomial FIR predictors, and optimum predictive power estimators developed by A. Huang. Also, linear AR predictors are designed for the task but they are found inadequate.

The simulators model the Qualcomm CDMA closed loop power control system which is found very restrictive by itself, not leaving much room for improvements by the predictive filtering. It is concluded that in this system, fine tuning the closed control loop is possible with proper predictive filtering.

Keywords: closed loop power control, mobile power control, code-division multiple-access, CDMA, predictive filtering, optimum power estimation, Heinonen-Neuvo polynomial predictor, multiuser communications system simulation

Preface

This work has been a most rewarding task, allowing me to reach into the world of mobile communications. This, along with learning concepts and tools of signal processing, has given me much valuable insight that I now can apply not only in the field of telecommunications but in most areas of engineering.

First and foremost, my thanks go to Prof. Iiro Hartimo, Lab. of Signal Processing and Computer Tech., HUT, for his great patience with my work, and most profoundly, for making the work possible altogether. He could be described as the Father behind me, and also, let me mention that he has had a very flexible mind in the matters like my conference travel plans. I would like to express my most sincere gratitude to Prof. Seppo Ovaska, Lab. of Electric Drives and Power Electronics, HUT, for his ever ready and remarkably profound coaching during these first steps on my path towards a scientific career. His work I have found most valuable; with his guidance, he has set me a standard for creating quality publications, and also for scientific work in general. These standards let me not ever forget. A glimpsing thought goes through my mind that this Thesis is probably written somewhat too fast to escape his red pen (but I'm not going to show this to him until after binding). Also, thanks are due to Prof. Timo Laakso, Lab. of Telecommunications Tech., HUT, for cooperation and guidance during the yearly stages of my work. Prof. Sven-Gustav Häggman, Communications Lab., HUT, is acknowledged for most kindly reading and commenting the Thesis. My many thanks extend to a coworker Lic.Tech. Aiping Huang, Lab. of Signal Processing and Computer Tech., HUT, for her guidance in many theoretical matters, and for her tirelessly ever friendly cooperation also otherwise. She never stopped smiling no matter how close our publication deadlines were. Research for this Thesis was carried out in parallel with hers, presented in her Licentiate Thesis [Hua97]. She has provided part of the predictors employed in the simulations presented here. For help in simulation matters, I am in debt to M.Sc. Jari Mattila, and thanks also go to M.Sc. Timo Korhonen and Lic.Tech. Michael Hall for many theoretical discussions in which they were always ready to take the time to make me understand several difficult things. All three are with Communications Lab. of HUT. Last but not least, I would like to thank the whole personnel of Laboratory of Signal Processing and Computer Technology for being a lively, very refreshing, and most friendly group in which I have found it fabulous to do scientific work. Let the spirit of Café Signal never fade, and let it inspire many generations of signal processing researchers to come.

Also, I would like to thank my parents, Sirkka and Raimo, for actively making sure that I had food and money during my studies and research, and for their support in general.

This work was funded by the Technology Development Centre of Finland, Nokia Corporation, Telecom Finland, and Helsinki Telephone Company, Finland. I was also supported through personal grants from the Päijät-Häme Fund under the Auspices of the Finnish Cultural Foundation, and from Foundation of Technology, Finland.

In Otaniemi, January 19, 1998

Jarno Tanskanen

List of Publications

All the Publications [P1], [P2], [P3], [P4] and [P5], are jointly referred to as *the Publications*.

[P1] J. M. A. Tanskanen, A. Huang, T. I. Laakso, and S. J. Ovaska, "Polynomial prediction of noise shaping Rayleigh fading," in *Proc. 1995 Finnish Signal Processing Symposium*, Espoo, Finland, June 1995, pp. 26–29.

[P2] J. M. A. Tanskanen, A. Huang, T. I. Laakso, and S. J. Ovaska, "Prediction of received signal power in CDMA cellular systems," in *Proc. 45th IEEE Vehicular Technology Conference*, Chicago, IL, July 1995, pp. 922–926.

[P3] J. M. A. Tanskanen, J. Mattila, M. Hall, T. O. Korhonen, and S. J. Ovaska, "Predictive closed loop transmitter power control," in *Proc. 1996 IEEE Nordic Signal Processing Symposium*, Espoo, Finland, Sept. 1996, pp. 5-8.

[P4] J. M. A. Tanskanen, J. Mattila, M. Hall, T. Korhonen, and S. J. Ovaska "Predictive closed loop power control for mobile CDMA systems," in *Proc. 47th IEEE Vehicular Technology Conference*, Phoenix, Arizona, USA, May 1997, pp. 934-938.

[P5] J. M. A. Tanskanen, A. Huang, and I. O. Hartimo "Predictive power estimators in CDMA closed loop power control," in *Proc. 48th IEEE Vehicular Technology Conference*, Ottawa, Ontario, Canada, May 1998, in press.

Contents

List of Abbreviations

Abbreviations are listed here as used in the introductory part of this Thesis. The abbreviations used in *the Publications* may be Publication specific, and are defined within each Publication.

AR	AutoRegressive
AWGN	Additive White Gaussian Noise
BER	Bit-Error-Rate
BPSK	Binary Phase Shift Keying
CDMA	Code-Division Multiple-Access
CIR	Carrier-to-Interference Ratio
COSSAP	Communications Simulation and System Analysis Program
DS	Direct Sequence
FFT	Fast Fourier Transform
FH	Frequency Hopping
FIR	Finite Impulse Response
GSM	Global System for Mobile Communications
HM	Hammerstein Model
H-N	Heinonen-Neuvo
IEEE	Institute of Electrical and Electronics Engineers, Inc.
IIR	Infinite Impulse Response
LOS	Line of Sight
LS	Least Squares
MDL	Minimum Description Length
MENN	Modified Elman Neural Network
MSE	Mean Squared Error
MUD	MultiUser Detection
NN	Neural Network
NSF	Noise Shaping Filter
PMDL	Predictive Minimum Description Length
PN	Pseudo Noise
QF	Quadratic Filtering
RF	Radio Frequency
SIR	Signal-to-Interference Ratio
SNR	Signal-to-Noise Ratio
SS	Spread Spectrum
WGN	White Gaussian Noise
WM	Wiener Model

List of Symbols

Symbols are listed here as used in the introductory part of this Thesis. The symbols used in *the Publications* may be Publication specific, and are defined within each Publication.

$\hat{\cdot}$	estimate of a quantity or signal
$\Delta\cdot$	shift or interval
$\cdot'$	quantity with a different value
$\cdot_c$	quantity referring to carrier, or to control command period
$\cdot_D$	referring to Doppler
$\cdot_i$	in-phase component of a signal, or referring to *i*th propagation path , or *i*th neuron input
$\cdot_q$	quadrature component of a signal
$\cdot_N$	quantity referring to filter of length, or order *N*
$\cdot_q$	quadrature component of a signal
$\cdot_r$	quantity referring to a received signal
$\cdot_t$	quantity referring to a transmitted signal
$\cdot_{long}$	long-term quantity
$\cdot_{\max}$	maximum of a quantity
$\cdot_{short}$	short-term quantity
α	angle between the mobile speed and transmitted radio wave
θ	phase angle
σ	square root of mean squared error, or square root of variance
τ	time interval
λ	wavelength
a	filter denominator coefficient
A	short term signal amplitude
b	filter numerator coefficient
C	number of context layer neurons
c	transmitter power level setting, or speed of light
d	control loop delay in chip durations, or physical distance
E	envelope of the received fading signal, or field strength
f	frequency, or activation function
f_D	Doppler shift
G	antenna gain
h	FIR coefficient
i	propagation path index
K	number of neural network inputs
k	summation index
L	polynomial degree, or number of neural network outputs
l	summation index, or propagation path length
M	number of filter denominator coefficients, or number of bits per control interval, or number of neuron inputs
m	summation index
n	discrete time sample index, or summation index
N	number of FIR, or filter numerator, coefficients
O	neuron output
P	power
p	probability density function
R	number of propagation paths
S	sequence length in samples
s	weighted sum of neuron inputs
t	propagation delay, or continuous time index
U	number of mobile users in a system
v	mobile speed
$\vec{v}$	mobile speed and direction
w	neuron connection weight
x	noiseless signal (the noisy counterpart is y)
X	processing block input signal sample value
$XCorr$	cross-correlation
y	noisy signal (the noiseless counter part is x)
Y	processing block output signal sample value, or radio channel output

1. Introduction

Always has communications played an important role in the history of mankind. Besides development of means of traveling, which actually can be considered to have been also the only means of data transport, it can be considered the single most efficient agent that has changed the views of vast numbers of people with methods ranging from continent-wide propaganda to very personal communications [Li95]. In the sense of reaching everybody on the globe, the modern communications is still far from being truly global but the growing commercialism requires more efficient communications technologies to keep on growing, and also the wireless communications technology itself is making itself affordable, desirable, and finally, indispensable. This technological evolution is investigated in [Sha97] and [Vit94b].

Increasing density of active cellular telephone users is a well-known problem in the field of mobile communications. With the existing systems, this has to be taken care of by network planning, and reorganizing the existing networks, for example, by reducing cell sizes in dense mobile user environments. It is well understood that a future mobile communication system should possess profoundly more user capacity in order to be successful. Direct-sequence spread-spectrum code-division multiple-access (DS/SS/CDMA) system technology is one of such new technologies which is already trying to penetrate the markets [Sch90], [Mag94]. Several differing analyses on the user capacities of CDMA systems have been conducted [Gil91], [Vit93b], [JaM94], [Lee97], [Ada96]. Although there are many opinions on the achievable user capacity increase, the importance of power control system in CDMA systems has been well established [Gil91], [Vit93a], [Sim93], [Vit95], [Vit94a], [Cam96]. It is generally accepted that the user capacity of a CDMA system is crucially interference limited, and thus the mobile power control function plays a major role in maximizing the capacity. The effects of imperfect power control are studied in [Pra92], [Kim97], and [Pri96].

The motivation for the work presented in this Thesis arises from these power control needs of mobile CDMA communications systems. In this Thesis, the power control system aims to maintain the received power levels from all the mobile users at equal and constant level at the base station receiver. This is one of the actual possible basis for the power control [Qua92]. The power control is to minimize the near-far effect [Lin92], i.e., the phenomenon that without proper power control mobiles close to the base station cause overly large interference levels to the reception of the users further away. Also, the power control systems should be able to counteract fast Rayleigh fading at least to the extend that the bit errors caused by the Rayleigh fading are randomized [Qua92], i.e., there are not many errors caused by the same long lasting and deep fade. This error randomization occurs when the mobile speed is sufficiently high, and the fades correspondingly of sufficiently short duration. Below that mobile speed, the power control systems should must be able to compensate for the fading in order to ensure sufficient transmission quality. In [Qua92], the field trials had shown that the power control, described in [Qua92], is able to compensate for fading at mobile speeds of 0 miles/h, …, 10 miles/h. At the speeds over 20 miles/h, the fades were short enough for the interleaver [Sim93] to make it possible for the Viterbi decoder [Vit95] to function properly. Within the mobile speed range from 10 miles/h to 20 miles/h, the power control system was not able to compensate for fading, nor was the errors sufficiently randomized in order to provide for good error correction performance.

Now, the aim of applying predictive lowpass filtering in a closed power control loop starts to unfold. First, the lowpass filtering itself is necessary in a systems which measures the received

power level, as otherwise also much of the noise power would be accounted into the received power level estimate causing severe received power level estimation errors. Secondly, closed control loop response is always delay limited. In the loop there are several sources of signal processing delays, as well as the radio propagation delays (estimation of propagation delays, [Str96]) both ways. Thus, it would be intuitively desirable to be able to predict radio channel behavior in advance so that the control action could be taken at a correct time despite of the control loop delays. Next, as mentioned, it is not helpful to try to maintain perfect power control above a certain mobile speed. Thus, the lowpass filtering could be designed so that the power controller would actually never need to see the fading which is too fast, and unnecessary for it to compensate anyway. In *the Publications* [P1], [P2], [P3], [P4], [P5], included into this Thesis, predictive filtering methods for improving received power level estimates are proposed and simulated. The received power level estimate is a naturally essential input to any transmitter power control system, and it is expected that any improvement in the quality of the received power level estimate directly contributes to the user capacity. The methods take advantage of any polynomial-like behavior, or of statistical properties in general, of the power response of a fading transmission path. Employing predictive polynomial estimation [Hei88] or optimum power estimation by A. Huang [Hua95], [Hua96], [Hua97], [Hua98], it is possible to reduce the effects of propagation and processing delays within a closed power control loop, and at the same time delaylessly reduce both interference and noise present in the received power level estimates.

In the first publications [P1], [P2], the predictability of radio channel power responses is investigated by applying predictive filters to noisy delayed Rayleigh fading signals. The noisy delayed Rayleigh fading signals are found well predictable, and criteria for selecting the right polynomial predictors for difference environments, i.e., for different noise levels and mobile speeds, are found. Next, predictors are employed into a closed power control loop of a single user CDMA communications systems [P3]. The results from the single user system are naturally not of great practical interest but they very clearly state the definite need for filtering in general within an interference, or noise, limited power control system. Finally, the system evolves into a full multiuser simulator [P4], [P5], with 5 or 10 users. In this context, also additive white[†] Gaussian noise (AWGN) multiuser interference model simulations are performed. It is seen that with the selected Qualcomm's power control system parameters [Qua92], the power control system is inherently very restrictive and does not leave much room for improvements from simple predictive filtering. Anyway, the results state that the closed power control loop can be fine tuned with proper predictive filtering.

[†] Note: The terms white Gaussian noise (WGN), and additive white Gaussian noise (AWGN), used in the Thesis and in *the Publications*, refer to Gaussian noise whose spectrum is flat within a limited frequency band determined by the sampling frequency, and zero outside this frequency band. Thus, WGN, and AWGN, can be associated with a finite variance.

2. Literature Overview

Calhoun [Cal88] gives a good, easy-to-read introduction to the field of cellular systems and after that Lee [Lee86] provides a somewhat more mathematical basic reading on mobile communication. [Eur93] is the GSM (Groupe Spécial Mobile, i.e., Global System for Mobile Communications) standard, and [Bai94] outlines third-generation mobile radio design issues. GSM is classified as a second-generation system. [Has93] is a tutorial-survey paper to indoor radio propagation issues. Among many other things, the classical Jakes' Rayleigh fading channel model is presented in [Jak74], and a comprehensive study of propagation models with recommendations is given in [IEE88]. [Par92] can be recommended for reading on mobile radio propagation channels. Propagation power-spectral theory is discussed in [Gan72] where, for example, typical power spectra for some antenna geometries are derived. A channel simulators are described in [Has79]. In the last of which, Jakes' Rayleigh fader [Jak74] is implemented using a microprocessor. Computer models for some fading channels are described in [Loo91].

In [Mag94], several concepts of spread spectrum (SS) systems are clearly stated. [Sim85] along with [Pic91] serve as more mathematical basic references to SS systems, and [Car86] is a course book on communication systems. [Sch90] is a plain English introduction to both direct-sequence (DS) and frequency-hopping (FH) SS systems. A code-division multiple-access (CDMA) system overview with power control analysis is given in [Lee91]. Definitely one of the main issues in CDMA systems is the system capacity which is also discussed in [Gil91] with reference to interference suppression. A feed back power control model for CDMA systems is presented in [Ari93] and signal-to-interference (SIR) based capacity analysis is continued in [Ari94]. [Åst87] serves as a general reference to adaptive feedback control. A SIR based power control algorithm for mobile-to-base station transmissions in a time-division multiple-access (TDMA) system is analyzed in [Cha94]. In [Gej92], the base station-to-mobile link power control in CDMA systems is discussed on the basis of carrier-to-interference ratio (CIR). CIR based optimum power control is analyzed in [Zan92], and CIR based analyses of centralized and distributed power control schemes are given in [Gra93] and [Gra94], respectively. Effects of imperfection in CDMA power control systems are discussed in [Pra92], [Kud93], [Pri96], and [Kim97]. Call blocking probability in terms of average number of users requesting service, i.e., Erlang capacity, in a power controlled CDMA system is analyzed in [Vit93b]. Other references on the effects of power control on CDMA system performance and capacity include [Mil92], [Kud92], [Kim93], [Vit93a], [Ton94] and [Vit94a]. Also, a variety of neural network based solutions to the problems of communications technology have been proposed in the literature. For example, multiuser detection (MUD) performance of neural networks in CDMA systems is compared to performances of conventional techniques in [Miy93]. Channel equalization using neural networks is proposed by Kechriotis [Kec94]. Channel equalization schemes are used at the receiver to decrease the effects of channel distortions, e.g. power signal fading and interuser crosstalk interference, and to recover the transmitted symbols. [Fre91] is a basic course book on neural networks.

[Par87], [Orf90], and [The92] serve as the starting points to digital signal processing methods. Heinonen-Neuvo (H-N) polynomial predictors, used in this work, are introduced in [Hei88]. The method for implementing the first or the second degree H-N predictors of any length with a fixed number of arithmetic operations is given in [Cam91]. A signal processing oriented view to Newton-type predictors is presented in [Ova91b]. Optimization of polynomial

predictors for any application specific prefilter is derived in [Laa93]. Extensions of the Newton's backward prediction algorithm to linear smoothed Newton and to median smoothed Newton predictors are introduced in [Ova91a]. The linear smoothed Newton predictors are further extended to recursive ones in [Ova92]. Cellular mobile system concepts are brought together with predictive filtering by application of polynomial predictors to predictive estimation of received signal power in mobile CDMA communications systems. This application is discussed in *the Publications* with illustrative simulations. Detailed statistical analysis on power prediction is carried out by A. Huang in [Hua95], [Hua98] and [P5].

2.1 Related Papers by the Author

In addition to *the Publications*, the author has been a minor co-author in a few papers related to the field of predictive power control. The research results presented in these papers are reviewed in the Thesis.

In [Gao96], Gao introduces a hybrid neural network (NN) approach to the received power level prediction problematics. In that paper, predictive minimum description length (PMDL) principle is employed in NN structure optimization. In [Gao97a], the predictive NN concepts are develop in to a NN structure with a context memory component, i.e., the NN is given an ability to remember the aspects of the inputs not only through the change of weights but also explicitly using non-processing memory neurons that feed information from upper layers back to the lower layers. The concepts of [Gao97a] are illustratively elaborated in [Gao97c], where Gao also gives the tedious derivations of the PMDL principle and its usage to NN structure optimization.

General NN theory still has many unknown components. In [Var97], Varone fills one of these. In this paper, frequency responses of some NNs, originally designed for prediction of Rayleigh fading, are estimated and analyzed. Even though the NNs as non-linear systems do not possess frequency responses in the common sense, it is possible to estimate input-dependent frequency responses for them. This work gives new tools for NN designers to understand the fundamental properties of NNs.

In [Hua98], Huang gives demanding derivations for the optimum power estimator based on the Wiener model with a complex-valued input. Also, simulation results applying the optimum power estimators in a single user mobile transmitter closed loop power control system are given.

3. Prediction & Power Estimation

3.1 Predictive Filters & Power Estimation

Generally, a prediction based on N past signal samples and M past predictor outputs is given [Orf90] by

$$\hat{y}(n+1) = \sum_{l=0}^{N-1} b(l)y(n-l) - \sum_{m=0}^{M-1} a(m)\hat{y}(n-m) \tag{3.1}$$

where n is a discrete time sample index, $b(l)$ and $a(m)$ are predictor coefficients, $y(n)$ is a noisy predictor input signal sample, i.e., in this work, a received power level measurement or component of the received complex-valued baseband equivalent signal, and $\hat{y}(n)$ is the corresponding predictor output. The noiseless counterpart of the signal $y(n)$ is denoted later by $x(n)$.

As the baseband equivalent signal concerned is complex-valued, there are three possibilities for predictive power estimation. The predictive filtering can be done using real-coefficient predictors either to predict the components independently with two predictors Fig. 3.1(b), or to predict the signal power as such with a single predictor, Fig. 3.1(a) [Hua95]. It is also possible to use complex-coefficient predictors to predict the complex-valued baseband signal [Har95]. From the analysis point of view, it is sufficient to consider here only the real-coefficient cases. The extension to the complex-coefficient predictors can be done if desired.

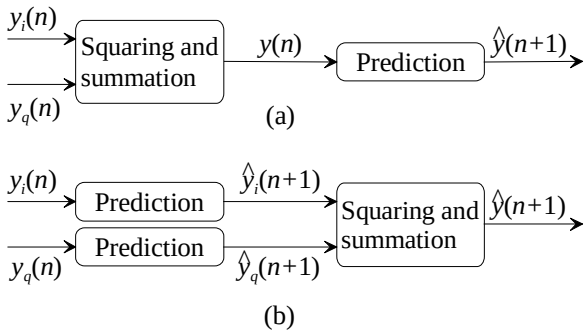

Fig. 3.1. Power prediction schemes for complex-valued signals. $y_i(n)$ and $y_q(n)$ are the noisy in-phase and quadrature components, respectively, $\hat{y}_i(n)$ and $\hat{y}_q(n)$ are the corresponding predictions, and $\hat{y}(n)$ is the prediction of the signal power.

3.1.1 Predictor Selection Criteria

In [P1] and [P2], the predictor selection criteria is the SNR gain achieved using H-N polynomial predictors with noisy, one-step-delayed Rayleigh distributed signals as inputs. The results are then used as reasonable choices for the predictors to be applied in the simulation setups in [P3] and [P4]. In this section, optimum H-N, and optimum power predictors for each mobile speed are found in a more consistent and unified manner. Two criteria, minimum mean squared error (MSE), and Minimum Description Length (MDL) criteria [Ris84], [The92], [Gao96], [Gao97] given by

$$\sigma^2 = \tfrac{1}{S}\sum_{n=1}^{S}\big(y(n)-x(n)\big)^2 \tag{3.2}$$

and

$$\mathrm{MDL}(N) = S\ln\sigma_N^2 + N\ln S\,, \tag{3.3}$$

respectively, are used for filter design parameter selection. In (3.2) and (3.3), $S = 2\ \mathrm{s}\cdot 9600\ \mathrm{samples/s}$ is the number of samples used in evaluating the criteria, $x(n)$ is the ideal predictor output signal sample, $y(n)$ the actual predictor output sample, and N the length or order of the predictor. The subscript N denotes that the quantity is calculated for the predictor of length or order N. MDL is actually a criteria used for finding the order of an autoregressive (AR) process [The92], and can also be used in determining the topology of neural networks [Gao96], [Gao97c]. As our Rayleigh fading process is not an AR process (cf. Section 4.3, Radio Channel Model), the MDL, or any other AR process order selecting criteria, cannot be expected to give exact results, and therefore it is always compared with the mean squared error criterion. The criteria are always evaluated using a different but statistically equivalent set of fading signal samples from that used in designing the predictors. Both criteria are evaluated over two seconds of Rayleigh fading channel power response for each noise level and mobile speed applied in the COSSAP simulations. The predictor design parameters over which the optimization is performed using MSE is given in [P5], except for the linear AR predictors which are shortly discussed in Section 3.1.4 below. The treatments in [P5] and in Section 3.1.4 are exactly analogous.

The Heinonen-Neuvo (H-N) and optimum predictors, reviewed below, are designed for the single user simulations for Rayleigh fading signal components with AWGN variances 0.1, 0.2, …, 0.9 for mobile speeds 10 km/h and 30 km/h, for 5 and 10 user simulations also for Rayleigh fading signal components but with AWGN variance 0.05, modeling receiver noise (and adjacent cell interference) and for mobile speeds 5 km/h, 10 km/h, …, 45 km/h, and finally, for the AWGN multiuser interference model simulations for fading signal components with AWGN variances of 1 and 5 for mobile speeds of 10 km/h and 30 km/h.

3.1.2 Heinonen-Neuvo Polynomial Predictors

As a class of finite impulse response (FIR) type predictors is considered in this work, the prediction (3.1) reduces to [Orf90]

$$\hat{y}(n+1) = \sum_{l=0}^{N-1} b(l)\,y(n-l)\,. \tag{3.4}$$

A filter of the form given in (3.4) is naturally inherently stable when $b(l)$ and $y(n)$ are bounded. With general infinite impulse response (IIR) predictors, given by (3.1), the stability would have to be separately proved in order to safely employ them in the closed power control loop. This is a natural requirement for the closed control loop to remain stable. To estimate a Rayleigh distributed signal by polynomials, the coefficients $b(l)$ are chosen to minimize noise gain when the predictor input signal is a low-degree polynomial corrupted by Gaussian noise. These predictors are generally know as Heinonen-Neuvo (H-N) polynomial predictors [Hei88], and have closed form predictor coefficients for given low degree of polynomial input signals. The coefficients $b(l)$ for the first and second degree predictors are given by

$$b_1(l) = \frac{4N - 6l + 2}{N(N-1)} \tag{3.7}$$

$$b_2(l) = \frac{9N^2 + (9 - 36l)N + 30l^2 - 18l + 6}{N^3 - 3N^2 + 2N} \tag{3.6}$$

where the subscript of *b* denotes the degree of the polynomial input signal for which the coefficients are optimized. From Fig. 3.2 it can be seen that the Rayleigh distributed signal piecewisely greatly resembles polynomials, and thus the approach is intuitively attractive. The Rayleigh fading prediction simulation results can also be interpreted as reflecting the amount of polynomial-like behavior of the Rayleigh fading signals. The Rayleigh signal in Fig. 3.2 is produced from the outputs of the noise shaping Rayleigh fader model in COSSAP, described later in Section 4.3.

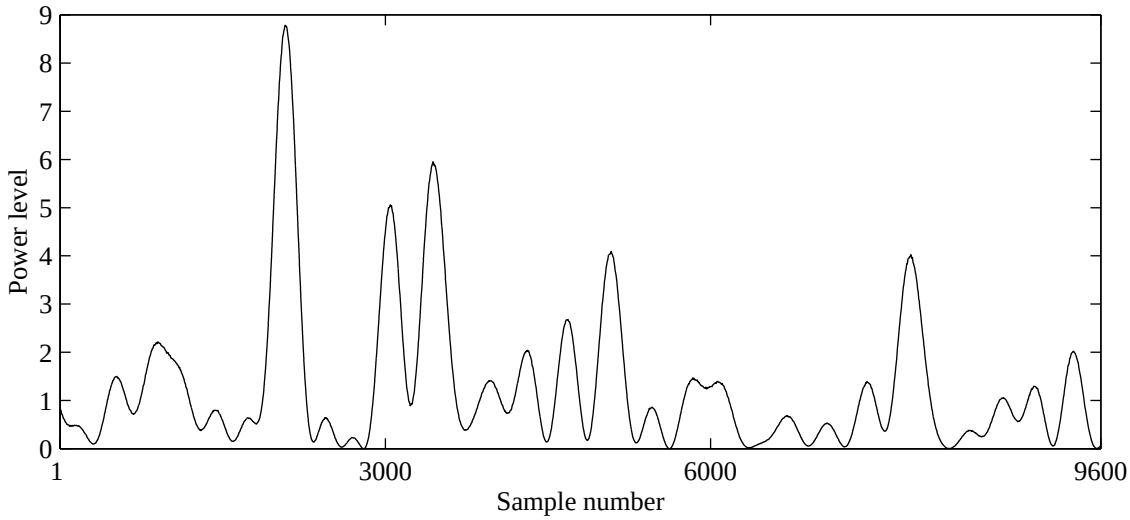

Fig. 3.2. One second of Rayleigh fading received signal power at the mobile speed of 10 km/h with the carrier frequency of 1.8 GHz.

To illustrate the prediction tools, some H-N predictor frequency and phase responses are shown in Figs. 3.3 through 3.6. The frequency responses of the first degree H-N predictors of lengths $N = 4, \ldots, 50$, and the group delays for the first degree, but lengths $N = 4, \ldots, 25$, within the frequency band of interest are more illustratively shown in Figs. 3.7 and 3.8, respectively. It is seen from Figs. 3.3, 3.5, and 3.7, that H-N predictors are lowpass filters with passband bandwidth decreasing with increasing filter length. As the polynomial degree is increased, the passband of the equally long predictors grows wider and also the passband peak increases. The prediction bandwidth, i.e., the frequency band within which the group delay is sufficiently close to -1, Figs. 3.4, 3.6 and 3.8, increases with the increasing polynomial degree. The prediction band in Figs. 3.4, 3.6 and 3.8 is actually seen to be quite narrow. This means that only the low frequency components of the Rayleigh fading signal power are actually predicted, the rest of the signal is more or less only filtered with a lowpass filter.

The MSEs and MDLs resulted of filtering a test Rayleigh fading signal component at 10 km/h, with added AWGN variance of 0.05, with H-N predictors of degrees $L = 1, 2$, and 3, and lengths $N = 4, \ldots, 50$, are shown in Figs. 3.9 and 3.10, respectively. The same results for mobile speed of 40 km/h are shown in Figs. 3.11 and 3.12, respectively. At 10 km/h, the

minima of MSE and MDL are found at first degree predictors of lengths $N = 40$ and $N = 39$, respectively, while at the higher speed of 40 km/h, Figs. 3.11, and 3.12, the optimum is reached at the filter degree two and length $N = 30$ for both MSE and MDL criteria. The sampling rate of the fading signal is 9600 Hz, and the carrier frequency 1.8 GHz.

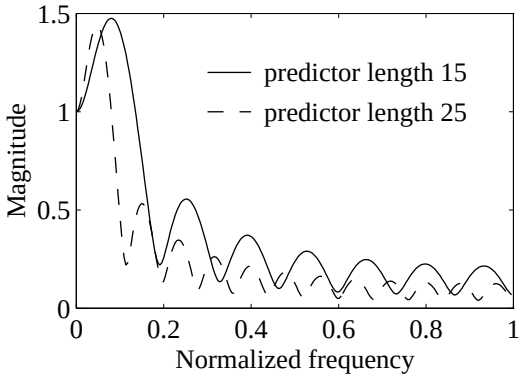

Fig. 3.3. Frequency responses of the 1st degree H-N predictors of lengths 15 and 25.

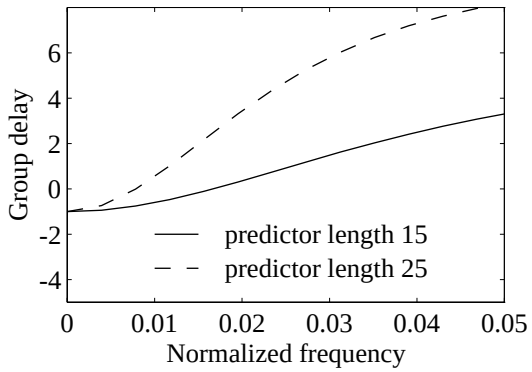

Fig. 3.4. Group delays of the 1st degree H-N predictors of lengths 15 and 25 (note the frequency scale).

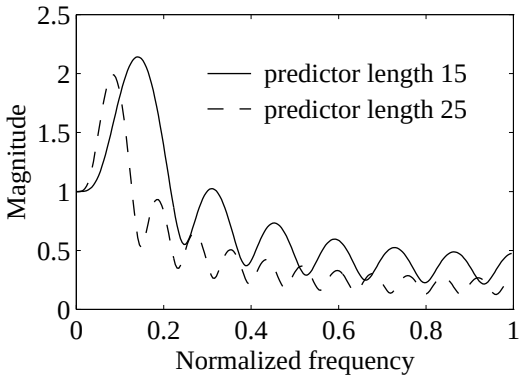

Fig. 3.5. Frequency responses of the 2nd degree H-N predictors of lengths 15 and 25.

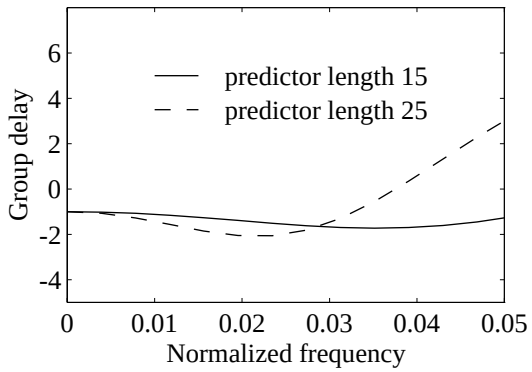

Fig. 3.6. Group delays of the 2nd degree H-N predictors of lengths 15 and 25 (note the frequency scale).

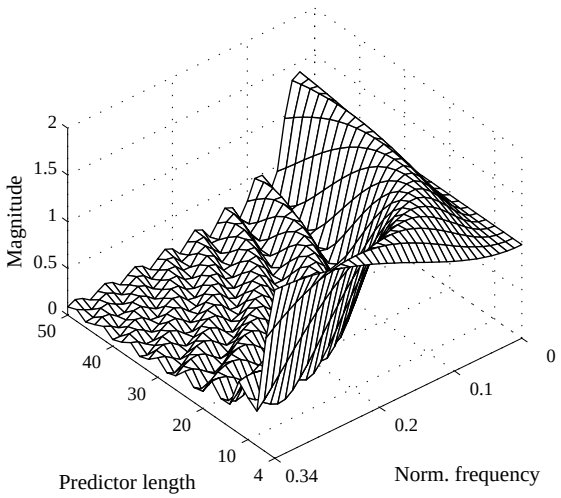

Fig. 3.7. Frequency responses of the 1st degree H-N predictors of lengths 4, ..., 50. Normalized frequency 0.34 is the maximum Doppler shift encountered in power signal at 50 km/h.

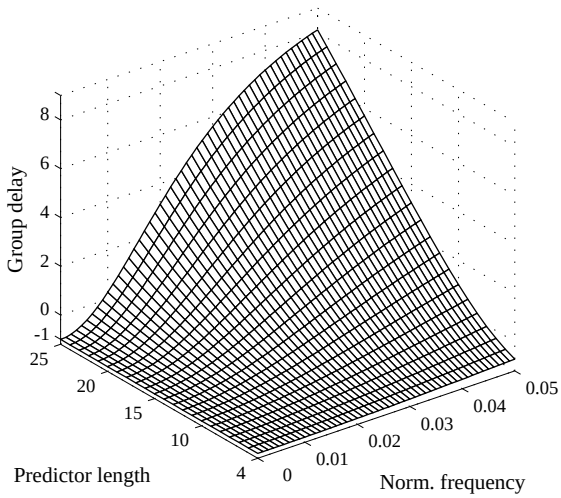

Fig. 3.8. Group delays of the 1st degree H-N predictors of lengths 4, ..., 25 (note the scales).

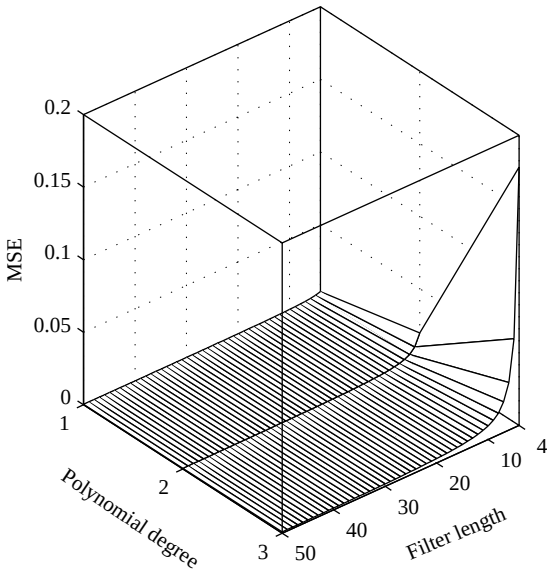

Fig. 3.9. MSE error surface for H-N predictors filtering the in-phase component of Rayleigh fading at 10 km/h with component AWGN variance 0.05.

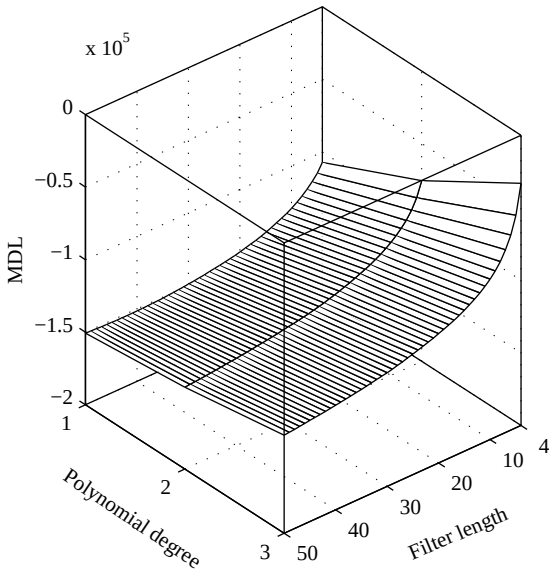

Fig. 3.10. MDL surface for H-N predictors filtering the in-phase component of Rayleigh fading at 10 km/h with component AWGN variance 0.05.

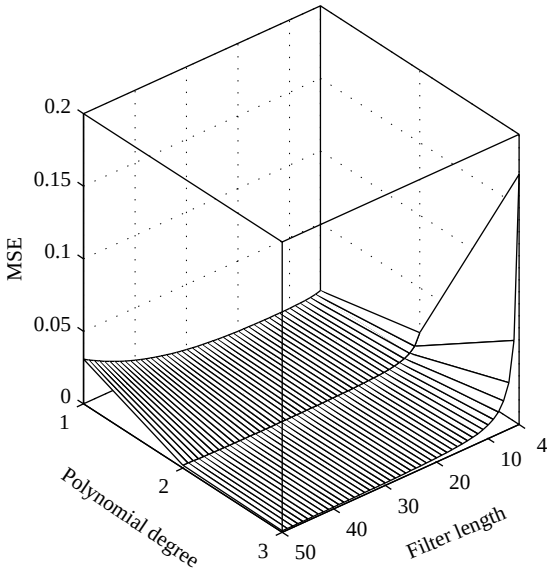

Fig. 3.11. MSE error surface for H-N predictors filtering the in-phase component of Rayleigh fading at 40 km/h with component AWGN variance 0.05.

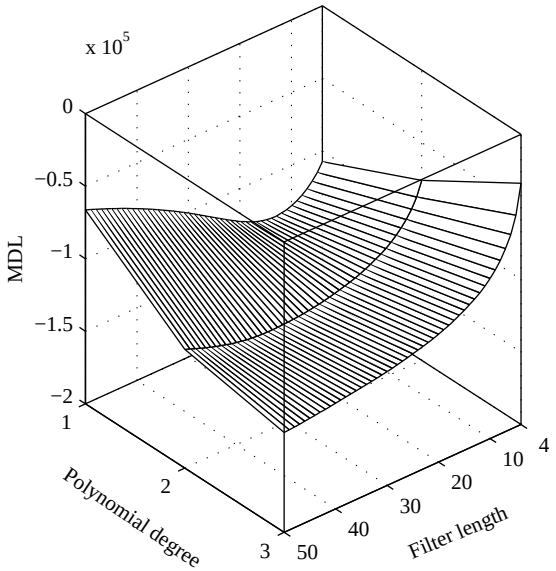

Fig. 3.12. MDL surface for H-N predictors filtering the in-phase component of Rayleigh fading at 40 km/h with component AWGN variance 0.05.

For further reading on predictive filtering, please, refer to publications of Ovaska [Ova], Laakso [Laa] and Ranta [Ran].

3.1.3 Optimal Power Estimators

Optimal power estimators based on both Hammerstein model (HM) and Wiener model (WM) are developed by A. Huang, and described and simulated in [Hua95a], [Hua95b], [Hua96a],

[Hua96b], [Hua96c], [Hua97] which is her Licentiate Thesis and a counterpart to this Thesis, [Hua98], and [P5].

General quadratic filtering (QF) [Pic82], [Sic92], [Fan95] is not well suited for practical real time application because of massive computations needed. Two simple structures [Fan95] of QF, HM and WM, with low computational requirements are of interests, though. Huang (see references above) has analyzed these models for complex-valued signals. A power estimator for complex-valued signals based on HM is illustrated in Fig. 3.1(a), and a WM based estimator in Fig. 3.1(b).

In WM based estimators, a global optimization yields a solution which is only applicable as numerical solutions for filter coefficients though iterative calculations. On the other hand, the estimator, Fig. 3.1(b) can be partially-optimized in closed form by solving for optimal estimation at the output of the filters, i.e., the overall power estimator is partially-optimized. For the results and derivations on optimum power estimators based on WM, please refer to [P5], or to [Hua98] in which the filter design more elaborately presented. Results in [P5] are achieved employing partially-optimized power estimators based on WM. HM based power estimator were not employed in the simulations presented in *the Publications*.

The predictor parameter selection method employed is described in [P5] with notes on the applicability to the power control problem at hand. Frequency responses and group delays of three of the resulted optimum predictors based on WM are shown in Figs. 3.13 and 3.14, respectively. The design parameters for the predictors, in Figs. 3.13 and 3.14 are selected according to the minimum MSE criterion. The minimum MSEs are found at predictor length $N = 50$ designed using 13200 prototype signal samples for 10 km/h case, at $N = 50$ designed with 15000 samples for 30 km/h, both with component AWGN variance of 0.05, and for 30 km/h with high component noise variance of 5, at length $N = 50$, designed using 2400 prototype signal samples. The optimum predictor designed for 30 km/h and noise variance of 0.05 possesses an actual prediction band, Fig. 3.14. The minimum MSE and MDL for 10 km/h, in Figs. 3.15 and 3.16, are both found with filter length 50 designed using 13200 prototype signal samples, while for 40 km/h, Figs. 3.17 and 3.17, the minimum is at filter length 24, designed using 15000 prototype signal samples for both criteria.

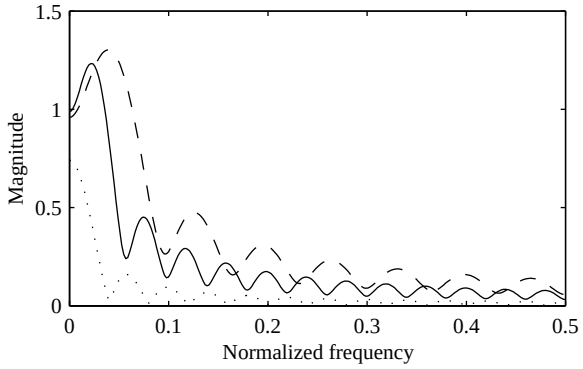

Fig. 3.13. Frequency responses of the optimum predictors designed for 10 km/h (solid) and 30 km/h (dashed) with component noise variance 0.05, and for 10 km/h and noise variance of 5 in components (dotted) (note that the frequency scale is up to half the Nyquist rate).

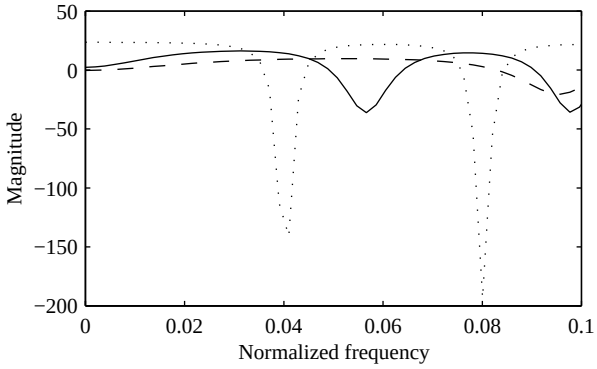

Fig. 3.14. Group delays s of the optimum predictors designed for 10 km/h (solid) and 30 km/h (dashed) with component noise variance 0.05, and for 10 km/h and noise variance of 5 in components (dotted) (note the frequency scale).

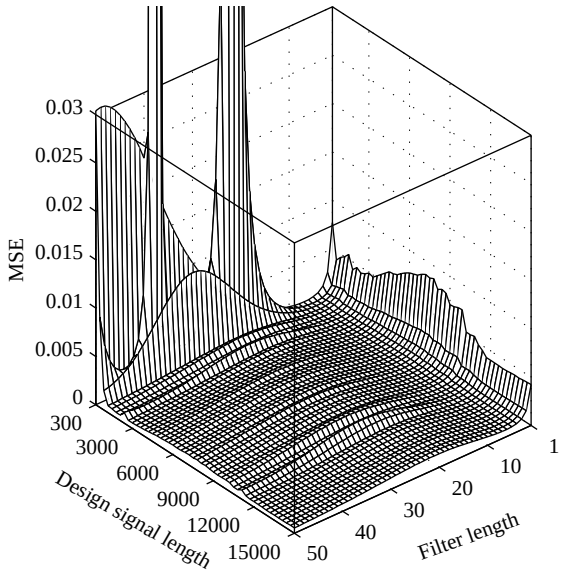

Fig. 3.15. MSE error surface for optimum predictors designed and tested with the in-phase component of the Rayleigh fading at 10 km/h with component AWGN variance 0.05.

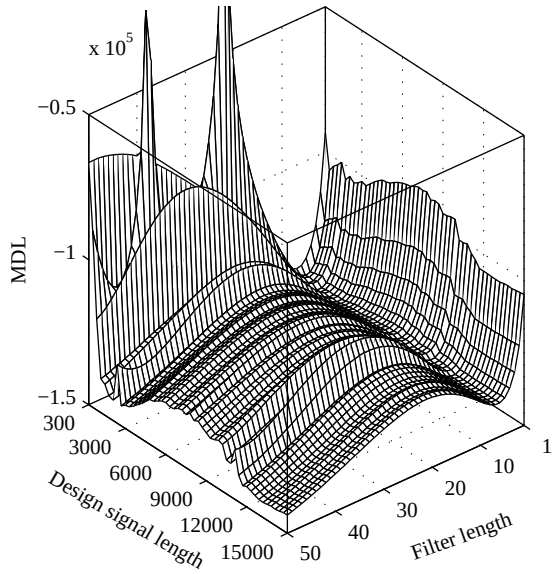

Fig. 3.16. MDL surface for optimum predictors designed and tested with the in-phase component of the Rayleigh fading at 10 km/h with component AWGN variance 0.05.

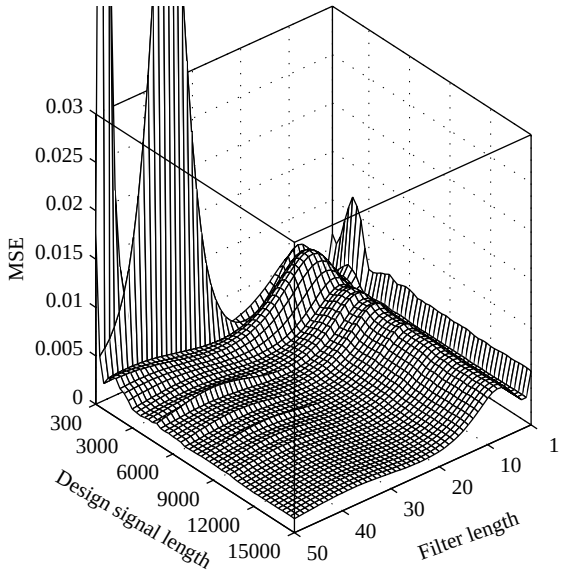

Fig. 3.17. MSE error surface for optimum predictors designed and tested with the in-phase component of the Rayleigh fading at 40 km/h with component AWGN variance 0.05.

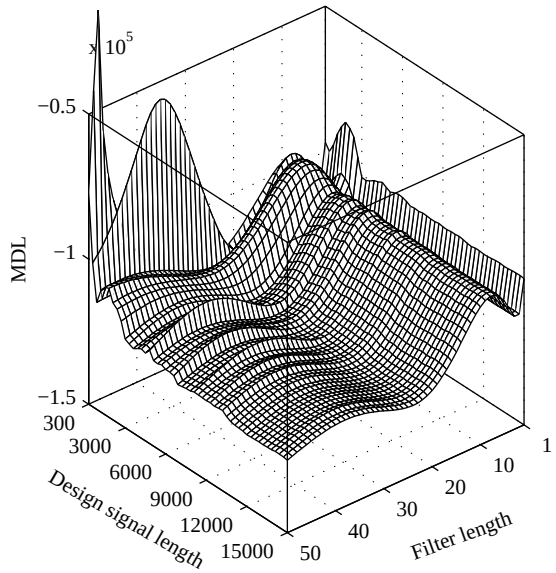

Fig. 3.18. MDL surface for optimum predictors designed and tested with the in-phase component of the Rayleigh fading at 40 km/h with component AWGN variance 0.05.

The fact that the filter coefficient optimization is performed for a predefined predictor length, results in that the prediction quality is to a large extend not dependent on the predictor length. This is seen as the large flat near-minimum MSE, and MDL, regions in Figs. 3.15 and 3.16, respectively. This property is less pronounced in the high speed case, illustrated by the MSE and MDL surfaces in Fig. 3.17 and 3.18, respectively. The nearly flat close-to-minimum regions in the MSE and MDL figures, Figs. 3.15, …, 3.18, actually mean that it is not necessary to perform strict optimization of the filters lengths and prototype signal lengths but little. This fact is employed in [P5] by designing optimum predictors with ad hoc selected

design parameters; length N=15, designed using 3000 prototype signal samples, i.e., predictors within the flat region, for each mobile speed and noise level. These predictors are then applied in all the same simulations presented for the optimum optimized predictors in [P5].

The results in [P5] confirm the above statement about the freedom to set the filter length and filter design prototype signal length. In [P5], it is seen that the simulation results do not greatly depend on whether the design parameters are optimized or selected ad hoc from the flat nearly-optimal design parameter region.

3.1.4 Linear Predictors

Originally intended as reference predictors for the research in this Thesis, also linear AR predictors are designed. Here the difficulty arises from the order selection [The92] of the predictor since in practice the actual order of the fading process would next to impossible to know accurately. In the simulations, the fading process is naturally known. The linear AR predictors are designed using the autocorrelation method [The92] with exactly the same filter design prototype signals as used for the optimum predictor design. The parameter selection method used in exactly analogous to that described in [P5] in Section II C.

MSE and MDL surfaces for 10 km/h and AWGN variance of 0.05 are plotted in Figs. 3.19 and 3.20, respectively. The minimum MSE is found at filter length N = 15, designed using 300 prototype signal samples, while MDL criterion yields the predictor of length one, designed also using only 300 prototype signal samples.

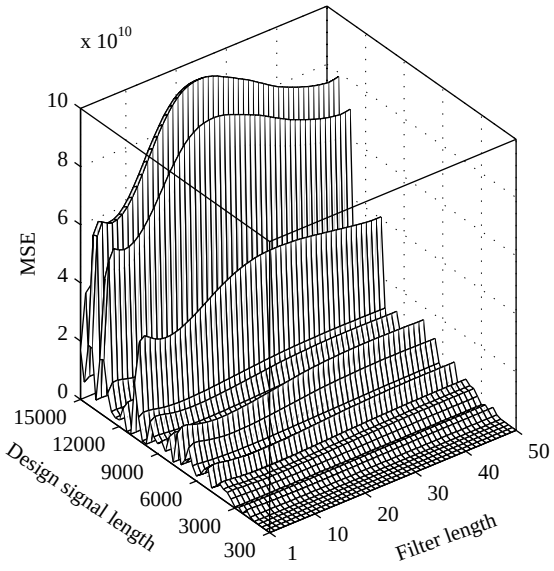

Fig. 3.19. MSE error surface for linear AR predictors designed and tested with the in-phase component of the Rayleigh fading at 10 km/h with component AWGN variance 0.05.

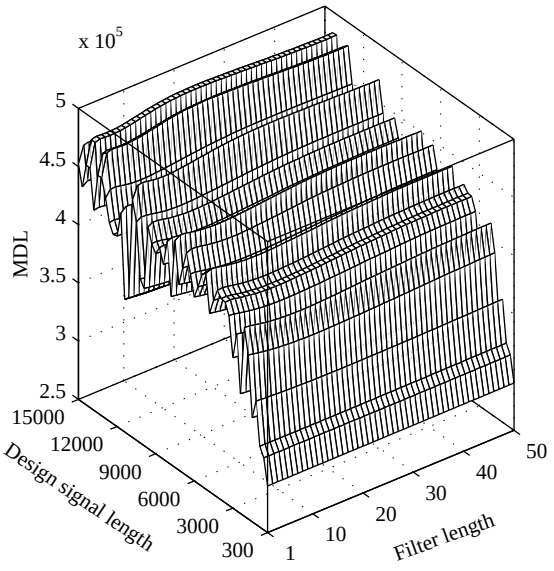

Fig. 3.20. MDL surface for linear AR predictors designed and tested with the in-phase component of the Rayleigh fading at 10 km/h with component AWGN variance 0.05.

The high MSE levels reveal that these predictors are not applicable to the problem at hand. Their frequency responses look actually worse than what could be considered decent to be shown here.

3.1.5 LS Optimal Predictors

Least squares (LS) optimal predictors [Kal85] are used as upper bounds for the performance evaluations with Rayleigh fading predictive filtering using H-N predictors in [P1] and [P2], in which also the applied LS predictor design principles are given.

4. Closed Loop Power Control Simulator

This chapter describes the latest and final version of the multiuser communications simulators constructed in COSSAP environment, and used to calculate the results in [P5]. In this chapter, mobile transmitter, radio channel, base station receiver, and power controller models, and their COSSAP implementations, are described in depth, also commenting on some implementation aspects arousing from COSSAP itself†. Partially similar system model concepts than simulated in this Thesis, are also described in [Cav97].

Simulators are constructed for both single user and multiuser systems, the difference of whose is evident in Section 4.4 Receiver Model. The presented single user system [P3] is of no practical value but the results serve as an introduction to the basic closed power control loop operation, which is many times is obscured in the multiuser system. The results very firmly establish the definite need for filtering in general within the closed power control loop. The multiuser simulator is an interesting system where several users, i.e., independent mobile station transmitters, are connected to a single base station. The users are individually power controlled, and interfere with each others. Adjacent cell interference and receiver noise is accounted for as added AWGN in the multiuser simulations. It would be easy to setup a multicell simulator, also. The multicell setup is described in Section 4.3 Radio Channel Model. Excluding actual system parameters, all parameters described with the respective component models are independently set for each user.

In the Figs. 4.1 - 4.3, 4.7, 4.9, 4.10, 4.12 and 4.13 below, all signal lines carry real-valued signals unless noted otherwise. A pair of signals originating from a common source and entering a common recipient forms a complex-valued signal.

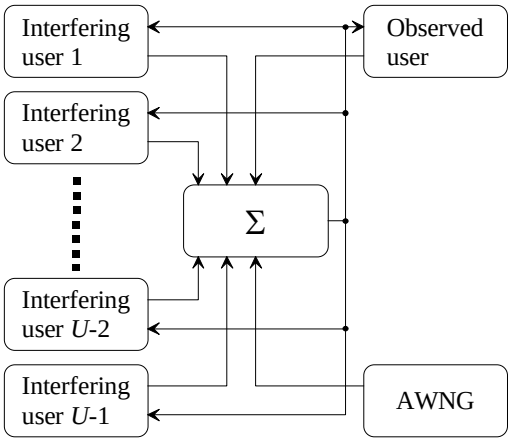

Fig. 4.1. Block diagram of a *U* user simulator. All the shown signals are complex-valued.

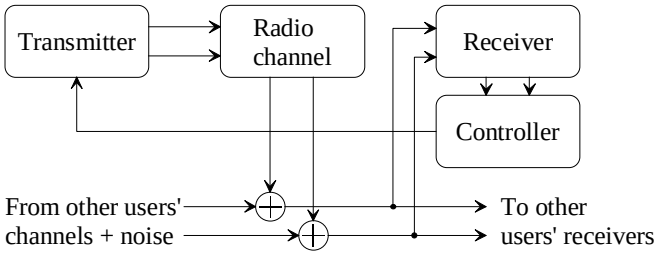

Fig. 4.2. Block diagram of a user component in Fig. 4.1. All the signals shown are real-valued.

† There exists a C-language-like number type casting feature in COSSAP, but the casting does not take the original variable type definition into account but type casting has to be done explicitly when using the parameter. The feature is that even though a COSSAP block parameter, say `$speed`, is defined to be a real number, and say, its value is a real variable divided by a constant, for example, `$speed=$mobile_speed/16`, were now the variables `$speed` and `$mobile_speed` are explicitly defined real in the design configuration, but `$mobile_speed` has an integer-like value, e.g. 10, and not 10.0, the division is carried out as integer division without type casting as expected by the design configuration variable definitions, and thus the result is truncated! The correct result is achieved for example by formatting the above parameter definition as `$speed=$mobile_speed/16.0`, which results in C-like automatic type casting. In this kind of simulation environment this can be considered a suspicious to say the least, especially as the variable definition does not cause type casting as should reasonable be expected. This feature may sometimes show up also as the reason for some unexplainable looking "divided by zero" errors when running simulations. Fortunately, none of the simulators used for *the Publications* was found to contain these truncation errors, though the "feature" was understood only at a very late stage of the research.

The overall picture of the multiuser simulator is shown in Fig. 4.1. Each user, Fig. 4.2, has its own independent transmitter, radio channel, receiver and controller components. A user transmits through his own radio channel to a common base station whose antenna sums the transmissions arriving from all the users along with some receiver noise and adjacent cell interference (the additive white Gaussian noise (AWGN) block in Fig. 4.1). The total noisy received signal is fed to each receiver, Fig. 4.2. In the multiuser simulators, after user detection, the receiver outputs the signal to the controller which makes power control decisions and sends power control command bits to the mobile transmitter accordingly.

In [P4] the chip rate is the same as in the Qualcomm system [Qua92] even though the number of chips per bit used is 127 while Qualcomm uses 128 bits per chip, whereas in [P5], the bit rate is set to 9600 bits/s, as with the Qualcomm system, resulting in a lower chip rate, while still using 127 chips per bit. Also, different seeds used in the random number generators for Rayleigh fading and AWGN generator have a little effect on the results, and thus the actual multiuser simulations give better results concerning H-N predictors in [P4] as compared to the corresponding results in [P5].

4.1 Uplink waveform

The CDMA link waveform actually used in the Qualcomm CDMA system [Qua92] is naturally somewhat more complicated than that employed in the simulations presented in this Thesis. Let us here shortly review the uplink waveform presented in [Qua92]. In that system, spreading is achieved using short pseudo noise (PN) codes of length 32768, generated with linear shift registers. The spreading code chip rate 1.2288 MHz provides for the chip rate of 128 chips per bit with data rate 9600 bits/s. Different mobile users are in turn distinguished at the base station receivers by the timing offset of a long PN sequence of length 2^{42}-1. Still, the data to be transmitted determines one of the 64 orthogonal Walsh functions which is transmitted combined with the short and long PN codes. In a multiuser CDMA system simulated in [P3], [P4] and [P5], users are detected according to the spreading codes which in the simulators are PN sequences of length 127 produced by linear shift registers. With the bit rate of 9600 bits/s, this results in the spreading rate of 1.2192 MHz employed in [P5]. In [P3] and [P4], the employed chip rate is 1.2288 MHz, and thus the bit rate is approximately 9675 bits/s.

Basis of the user detection in the presented simulators is the orthogonality of the codes, i.e., the crosscorrelations of different users' PN code sequences should be equal to zero. In the simulators described in this Thesis, interuser interference is introduced by generating the PN spreading codes of lengths 127 with shift registers with user specific initializations, since this choice for the spreading codes does not yield orthogonal codes but the correlation matrix, with the autocorrelations on the diagonal, is given by

$$XCorr = \begin{bmatrix} 127 & -1 & \cdots & -1 \\ -1 & 127 & \ddots & \vdots \\ \vdots & \ddots & \ddots & -1 \\ -1 & \cdots & -1 & 127 \end{bmatrix}. \tag{4.1}$$

In the literature, several different spreading code schemes are proposed for CDMA multiple access communications, for example [Vaj95], [Ban96], and [Lin97].

4.2 Transmitter Model

Block diagram of the mobile transmitter module, including also the transmission level setting logic, is shown in Fig. 4.3. The data to be transmitted is differentially encoded, and binary phase shift keying (BPSK) is applied [Jak74], [Car86]. Somewhat similar transmitter and receiver constructions as used in this Thesis are presented in [Cav97]. After BPSK, each BPSK block output sample is repeated for the number of chips per bit times. The sampling rate after the "Repeat for bit period" block is thus equal to chip rate. Next, the signal is spread by multiplying it with a user specific spreading code consisting of "-1"s and "1"s. Finally, transmission level is set by multiplying the signal by a power control multiplier. In the beginning of the simulation, the block "Control loop delay" produces d samples with the value $10^{-1/20}$, corresponding to the smallest possible transmission level. Subsequent transmission level settings are thus delayed by d chip periods. The total control loop delay d is realized here in order for it to effectively by the delay of the application of the power control action with respect to the channel fading. The delay d is set individually for each user, and accounts for all the loop delays, i.e., mobile and base station processing delays, and both uplink and downlink propagation delays. Also, in the beginning, a single sample with the value $10^{-1/20}$ is produced in the block "Produce on sample $10^{-1/20}$" which is multiplied by one generated by the "Produce one "1" to start loop" block, thus generating the first transmission level setting to be used in the transmission, which is repeated the number of chips per control period times to generate one sample for each transmitted chip. The transmission is thus always started using the lowest transmission power level. The production of the single samples in the beginning is necessary as COSSAP is a stream driven simulator, i.e., processing is done when all the necessary input samples are available. This means that getting the multiplicative transmission power level setting generation loop running, and also to start the overall closed power control loop, the described producing of the single samples within the loop is necessary. This also sets specific requirements for the placement of the control loop delay block. As it is the control action delay that is to be investigated, the delay has to be placed respective to the faded signal received at the base station. A COSSAP delay block generally operates so that N samples with a given value are generated before the input signal is passed through. These N samples are generated regardless of whether there are samples available in the input or not; this sample generation function is the property that actually makes it possible to get a simulator with a closed loop to run at all in a stream driven simulator like COSSAP. Placing the total loop delay block as shown in Fig. 4.3, when the simulation is started there is no power control action for the first d chip durations, and the control actions taken later are actually done based on the channel fading characteristics d chip durations in the past as desired. After the first d chip durations, for the first actual control period the transmitter power is kept at the minimum, and thereafter altered ±1 dB [Qua92] according to power control command bits received for the controller in the base station. The ±1 dB transmission level change step implies that the next transmission level setting is always generated from the last one by multiplying that with $10^{1/20}$ or $10^{-1/20}$, respectively. A single power control bit is received in the beginning of every power control period. The "Limit" block sets the dynamic range of the power control to ±15 dB from the nominal 0 dB. For the equations concerning the transmitter setup, please, cf. [P3], [P4]. In Fig. 4.3, also the different signal sampling frequencies are shown with different line types. Having three different sampling frequencies within the simulator also requires extra care for correct signal timings within the stream driven simulator.

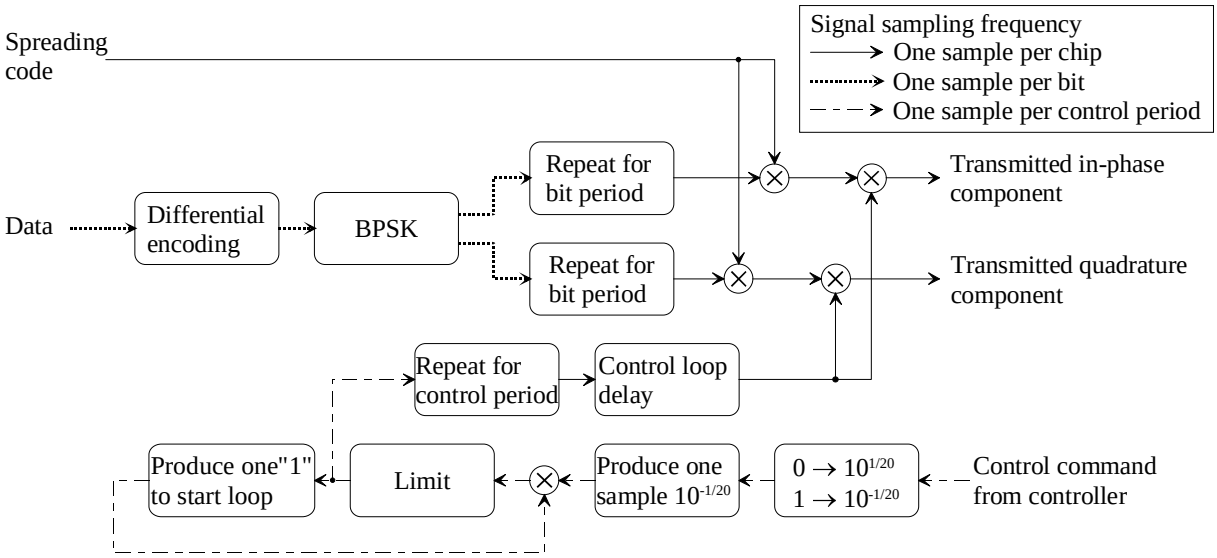

Fig. 4.3. Block diagram of the transmitter with transmitter power level setting generation. Different signal sampling frequencies are shown with different line types. The notation $X \rightarrow Y$ denotes that for each input sample with a value X, a single output sample with value Y is generated.

4.3 Radio Channel Model

Several phenomenon disturb radio transmissions in radio channels [Jak74], [Lee86], [IEE88], [Par92], [Eur93]. Distance and natural objects, like hills and forests, between a transmitter and receiver cause long term fading in the signal power. Mainly unnatural obstacles, like cars and buildings, in the radio propagation path reflect signals causing several attenuated echoes of the same transmitted signal to arrive at the receiver with different delays in different phases after traveling over different distances. This is the cause of short term fading, also called fast fading. As the mobile unit moves, the Doppler effect causes frequency shifts that may be different for each multipath component. Furthermore, the mobile speed is generally not constant, and also some of the unnatural obstacles are in constantly changing motion. These effects are illustrated in Fig. 4.4, which also illustrates the different phases of the received multipath components.

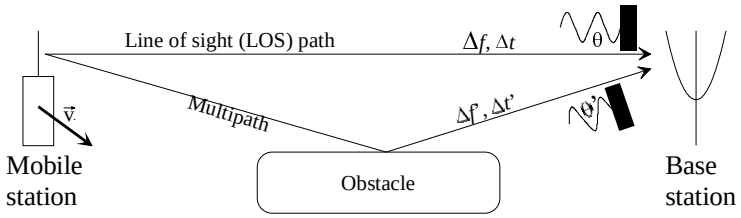

Fig. 4.4. Two multipath components arrive at the base station receiver with different Doppler frequency shifts Δf and $\Delta f'$, propagation delays Δt and $\Delta t'$, and phases θ and θ'. The mobile station is moving with the speed and direction $\vec{v}$. Also, the obstacle might not be fixed, and all the variables are generally time dependent.

Many different radio channel propagation models have been proposed to account for different channel properties. Different channel models are designed for different environments and communications systems. There exist models for rural areas, hilly terrain, urban areas, etc. [Eur93]. In general, channel properties are both frequency dependent and functions of time. The time interval over which the channel response remains approximately constant is called

the coherence time, and the frequency separation over which two signals are correlated enough is called the coherence bandwidth. The correlations to decide the coherences are to be set according to the problem at hand.

The distance between a base station and a mobile phone determines the propagation path loss in free space. This propagation path loss is only function of distance d and carrier frequency f_c [Par92], and the received-to-transmitted power ratio is given by

$$\frac{P_r}{P_t} = G_t G_r \frac{c^2}{\left(4\pi d f_c\right)^2} \tag{4.2}$$

where P_t and P_r are transmitted and received power, respectively, and c is the speed of light. G_t and G_r are the gains of transmitting and receiving antennas, respectively. The received fading signal $E(t)$, i.e., the field strength in dB in reference to a known field strength in volts/meter, is the envelope of the received radio-frequency (RF) signal. It can be modeled as being composed of a long-term fading signal $E_{long}(t)$ and of a short-term fading signal $E_{short}(t)$ [Lee86] as

$$E(t) = E_{long}(t) \cdot E_{short}(t) \,. \tag{4.3}$$

The long-term fading signal is the envelope of the received fading signal, and can be calculated from the whole fading signal as a local mean over a suitable time interval. An estimate of the local mean is given by

$$\hat{E}_{long}(t) = \frac{1}{2\Delta t} \int_{t'-\tau}^{t'+\tau} E(t)dt \tag{4.4}$$

where τ is the time interval to be chosen according to the fading characteristics. The long-term fading can also be considered to be a function of distance instead of time for path loss calculations. The problem of local mean signal strength estimation is considered in also in [Val97].

The appearances and relative amplitudes of these two fading effects depend on the environment. Fast fading is more evident in man-made environments whereas long-term fading is mostly due to landscape and line-of-sight (LOS) distances. It is not possible to define an exact frequency separating these two fadings since the long-term fading may occasionally also contain high frequency components usually encountered in fast fading signals. This happens when the non-reflected path, i.e., LOS path, is abruptly lost, for example. A radio channel with a band-limited fixed-average-power input signal, no fading, and thermal noise as the only disturbance, may be approximated by an additive white Gaussian noise (AWGN) channel [Car86]. The AWGN channel is specified as a distortionless transmission channel with a fixed bandwidth. In this model, the transmitted signal is contaminated by additive bandlimited zero mean white Gaussian noise with fixed average power. The signal and the noise used are independent so that the received signal sample is the sum of corresponding transmitted signal and noise samples, and the received average total power is the sum of average powers of the transmitted signal and the noise.

In most real environments a radio signal propagates from transmitter to receiver via many different paths, as mentioned earlier. Naturally, situations with one dominating path are possible. Different paths are caused by environmental reflectors, for example by buildings and vehicles. This multipath phenomenon causes a variety of difficulties: different paths exhibit different attenuation, the length of each path is different causing several copies of the transmitted signal to be received after different time delays with different phases and the velocity of the mobile unit to the direction of different paths is different causing each multipath component to experience different Doppler shift. When the receiving antenna sums these dispersed copies of the signal, the signal is understandably severely mutilated. In general, all these effects are time and frequency dependent, i.e., time- and frequency-selective, respectively.

Multipath propagation causes fast fading, which is also called Rayleigh fading. Assuming that the received signal consists of a large number of components with random phases, the probability density function of the signal envelope follows Rayleigh distribution that is given by

$$p(A_i) = \begin{cases} \frac{A_i}{\sigma^2} e^{-A_i^2/2\sigma^2}, & x \geq 0 \\ 0, & x < 0 \end{cases} \tag{4.5}$$

with the mean power σ^2 and short-term signal power $A_i^2/2$. Considering the signal wavelength of, for example, about 30 cm at 1 GHz, and comparing that with changes in path lengths when the transmitter is in a moving car, it can clearly be understood that the phases of the copies of the signal arriving through different paths are rapidly changing and can thus be considered random with even distribution.

In a stationary transmission setup, i.e., when neither the receiver nor the transmitter is moving and their environment is constant, the received signal is a sum of delayed copies of the transmitted signal, with a different attenuation associated with each path, given by

$$Y(t) = \sum_{i=0}^{R-1} A_i y(t - \Delta t_i) \tag{4.6}$$

where $Y(t)$ is the output of the whole channel at time t, $y(t - \Delta t_i)$ is the copy of the signal arriving through the ith path with delay Δt_i, A_i is the attenuation associated with the ith path and R is the total number of paths. If the system is not stationary, amplitude coefficients, delays and the number of paths may be time varying. Even if the system is completely stationary the copies of the signal reach the receiver in different phases according to the lengths of the paths. Given the length difference of two paths as $\Delta l(t)$, the phase difference is given by

$$\Delta\theta(t) = 2\pi\Delta l(t)/\lambda \tag{4.7}$$

where λ is the wavelength. In addition, if the mobile unit is in motion the transmitted frequency suffers from a Doppler shift

$$\Delta f(t) = v\cos\alpha(t)/\lambda \tag{4.8}$$

where v is the speed of the mobile unit and $\alpha(t)$ is the angle between the direction of the mobile speed and the transmitted wave. From (4.8) it can be seen that the maximum increase in frequency is encountered while the mobile is moving directly towards the base station and the maximum decrease while moving straight away from the base station. In (4.7) and (4.8) the original transmitted frequency and the speed of the mobile are considered constant, but in practice they may be time dependent as well.

Including all these effects and considering R resolvable multipath components, each composed of M waves with possibly different delays Δt_{nm} arriving at the receiver with equal Doppler shifts f_{Dn}, the received signal can be modeled as [Jak74]

$$E(\omega,t) = E_0 \sum_{n=1}^{R} \sum_{m=1}^{M} A_{nm} \cos\left(f_c t + f_{Dn} t - f_c \Delta t_{nm} \right). \tag{4.9}$$

Differing delays cause phase distortion $f_c \Delta t_{nm}$ of the signal. The original transmitted frequency is f_c, and E_0 is the amplitude of the transmitted signal. Coefficients A_{nm} reflect different signal power attenuation associated with each wave. In all practical cases each parameter in (4.9) is, at least in principle, time dependent. Effects of multipath on CDMA cellular communications are analyzed in [JaH94] and [Cha94], and estimation of propagation delays Δt is considered in [Str96].

Naturally, the channel simulator should produce as realistic power responses as possible. Minimum model input parameters are the mobile speed and carrier frequency, or the input signal envelope, or the actual transmitted waveform. It would also be of interest that the model could produce different channel responses according to the environment type, like urban area, given as an input. Predictors could also be designed using real measurement data but the resulting predictor would probably be too environment specific with no capabilities to function under a wider range of conditions but only in the conditions close to those of the measurements used.

In this work, the channel model employed is a single Rayleigh fading propagation path contaminated by additive white Gaussian noise (AWGN), and it is presented in the base-band. Now in (4.9) $R = 1$, and A_0 is Rayleigh distributed with AWGN added independently to the quadrature components. The AWGN presents receiver noise. The assumption on Rayleigh distributed received signal power is valid on a narrow-band communications systems, but not generally in CDMA systems. A CDMA the radio channel model consisting of a single Rayleigh fader would be overly pessimistic since because of the wide transmission band the fading cannot be considered frequency flat, i.e., the fading is frequency depended. Thus, some power is always available at some portion of the wide transmission band. A RAKE receiver [Pri58] is capable of distinguishing between different paths with sufficient delay separation. Implicitly including a good enough RAKE receiver within the radio channel model results in a single Rayleigh fader channel model to be seen through a single RAKE finger. Within the work presented here, RAKEs are not explicitly employed because the intention is to clearly see the effects of applied predictive filtering, and multipath combining, even though it would give better BER results in the simulation, would very probably obscure the results at least to some extent. Also, employing RAKEs would also mean employing actual multipath radio channel models into the simulations. But, as mentioned, the single Rayleigh fader channel model assumption can be considered to implicitly include a RAKE receiver. Performance of

RAKE receivers with random spreading sequences is analyzed by Cheun in [Che97], and a decision-directed SS RAKE is presented in [Pov96].

4.3.1 Jakes' Rayleigh Fader

In [P2] the Jakes' Rayleigh approximation [Jak74] is employed. In the Jakes' Rayleigh fader the Rayleigh distributed signal is approximated by sums of appropriately chosen sinusoids whose frequencies correspond to the Doppler shift frequencies [Jak74]. Jakes' Rayleigh fading model is further improved in [Den93].

4.3.2 Noise Shaping Rayleigh Fader

One other way to generate a signal whose amplitude distribution follows Rayleigh distribution is by summing two independent squared zero mean white Gaussian (WGN) noise processes [Car86]. The noise shaping Rayleigh fader, with also signal power calculation shown, is illustrated in Fig. 4.5. Since only the baseband equivalent signals are considered, the carrier mixer is not shown. The subscript "*i*" denotes the real part, i.e., the in-phase component, and the subscript "*q*" the imaginary, i.e., the quadrature component of the complex-valued baseband equivalent signal, and "$(\ )^2$" denotes squaring operation. The baseband equivalent signal components are formed by filtering two independent WGN processes by two identical but separate noise shaping filters (NSF) which are chosen according to the antenna geometry selected to be analyzed [Gan72]. The shaped noise sequences are then squared and summed to produce the Rayleigh fading signal power. Receiver noise and adjacent cell interference are simulated by adding zero mean additive white Gaussian noise (AWGN) to the in-phase and quadrature components independently before the squaring operation. In the simulations, the NSF approximates the received spectrum $S(f)$ given theoretically by [Jak74] as

$$S(f) = \frac{1}{\sqrt{1-\left(\frac{f-f_c}{f_{D\max}}\right)^2}}, \tag{4.10}$$

where f is frequency, f_c is carrier frequency and $f_{D\max}$ is the maximum Doppler shift frequency. The relations between spectra and antenna geometries are analyzed in [Gan72]. In [P1], the maximum Doppler shift frequency is derived from the vehicle speed which is set to either 5 km/h or 50 km/h, corresponding to the slow and high urban speeds, respectively, and the carrier frequency is set to 1800 MHz. As any filter with frequency response corresponding to the power spectrum of the antenna is suitable as the NSF, a 4000 tap FIR was designed to provide a good enough approximation of the desired frequency response [P1]. It was verified that the frequency responses closely matched the corresponding theoretical spectra for a vertical omnidirectional antenna. Before demodulation the spectrum is centered at the carrier frequency. At demodulation it is shifted to baseband, and centered at zero frequency.

In the standard COSSAP Rayleigh fader block, a fixed narrow-band lowpass NSF ("Spectrum shaping IIR" in Fig. 4.7) is used, and an interpolator takes care of the mobile speed and carrier frequency settings. In the original COSSAP Rayleigh fader model, two interpolators are used to achieve the correct interpolation ratio with the GSM system parameters. With the system

parameters applied here, a single interpolator is sufficient, though. The COSSAP NSF frequency response along with the theoretical response for an omnidirectional monopole antenna [Gan72], [Jak74] (4.10) is shown in Fig. 4.6. The NSF cutoff frequency, 0.00904956 in normalized frequency scale, and the NSF gain along with the set variance of the source WGN, are set so that the average power of the fader output signal can be set by simple multiplication by the desired average power setting, Fig. 4.7.

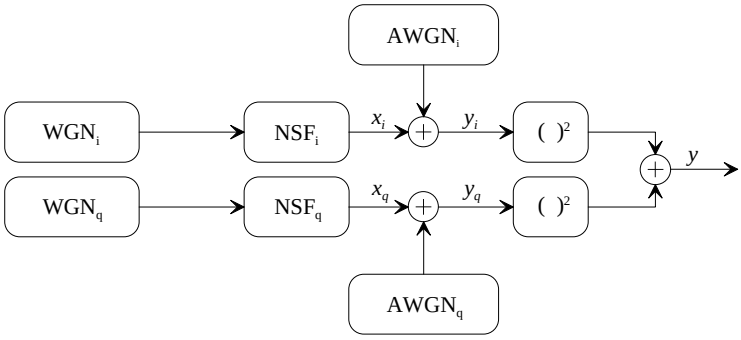

Fig. 4.5. Noise shaping Rayleigh fader. WGN is a white Gaussian noise process, AWGN is an additive WGN and NSF is a noise shaping filter.

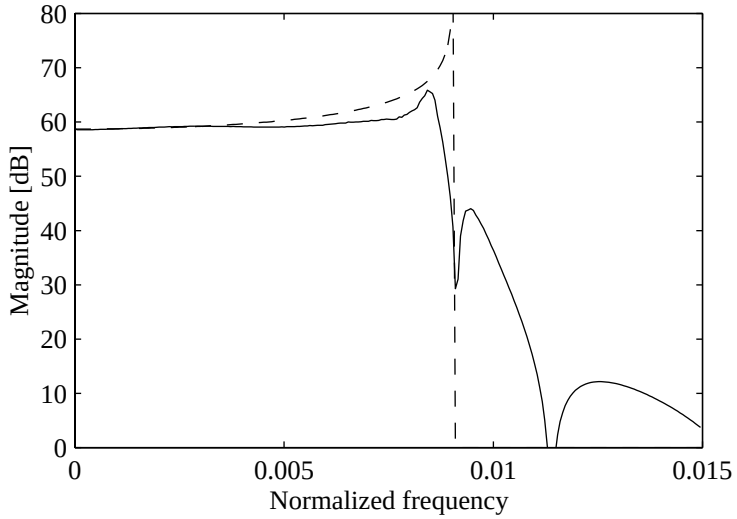

Fig. 4.6. Frequency response of the COSSAP Rayleigh fader IIR NSF (solid) along with the corresponding theoretical response (4.10). The theoretical response is scaled to have DC gain equal to that of the COSSAP NSF.

The radio channel model used in the simulations [P3], [P4], [P5], Fig. 4.7, is a single tap Rayleigh fading channel model in which Rayleigh fading is generated by noise shaping. First, a complex white Gaussian noise (WGN) signal is generated. The spectrum of the noise is shaped by a noise shaping filter. The filter is a standard COSSAP block and is selected so that the resulting noise spectrum corresponds to that seen by a single omnidirectional monopole antenna at the base station receiver. The passband width of the filter is set so that the final fading bandwidth, determined by the carrier frequency and mobile speed, can be set by interpolating the signal. After spectral shaping, the average fading signal power is set, and some first samples are deleted in order to allow for the noise shaping filter to settle. Finally, linear interpolation is applied to yield a correct fading signal bandwidth, and the fading is

applied to the transmitted signal. The output fading power of the Rayleigh fader in Fig. 4.7, is illustrated in Fig. 4.8.

Each mobile has a fading channel of its own, and the mobiles interfere with each other also through these same channels. This corresponds to the case where all the mobiles are connected to the same single base station. This single cell system can easily be changed to a multicell setup by introducing one radio channel per user per cell for adjacent cell interference, in addition to the different channel for intracell interference and transmission.

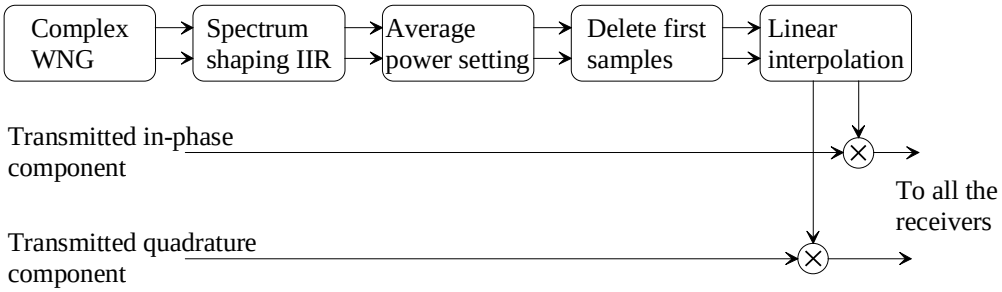

Fig. 4.7. Block diagram of the Rayleigh fading channel model.

The main difference between the Jakes' and the noise shaping Rayleigh faders is the frequency distribution. In the Jakes' fader, there is a number of distinct frequency components, carrying also all the signal power. On the other hand, in the noise shaping fader, the signal power is theoretically continuously distributed. Filtering the fading signal with a lowpass filter whose passband edge is close to the fading signal bandwidth, naturally distorts the signal, and in the case of the Jakes' fader, the distortion close to the maximum Doppler frequency frequency component may have a major effect on the power contained within the fading signal. With the noise shaping fader, this effect is not as severe.

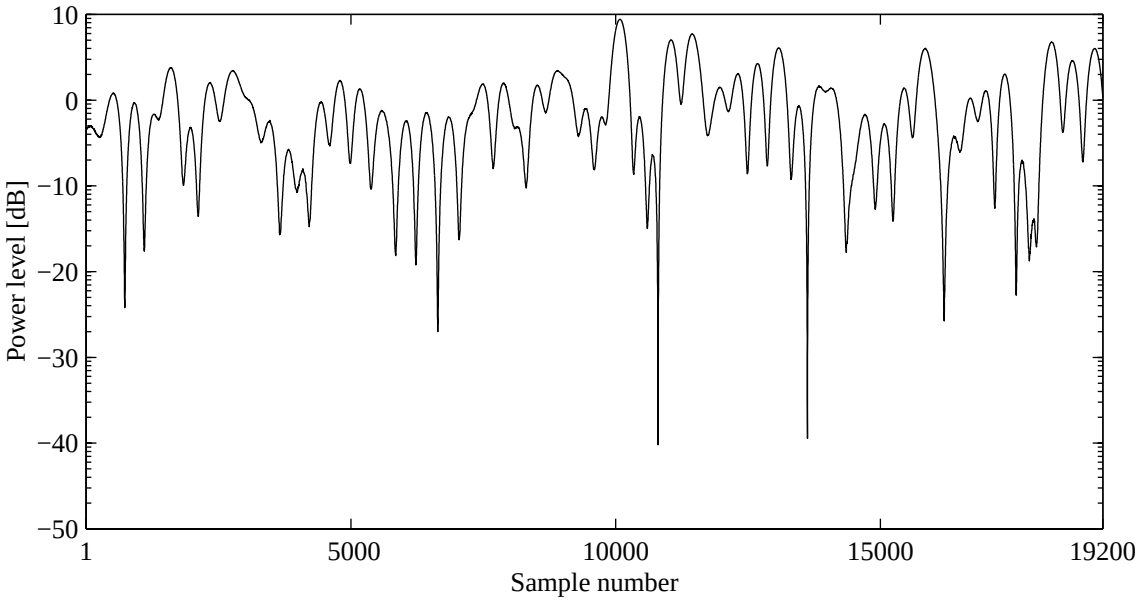

Fig. 4.8. Two seconds of the power of the Rayleigh fader output, i.e., the sum of squares of the "Linear interpolation" block outputs in Fig. 4.7, at mobile speed of 10 km/h, carrier frequency 1.8 GHz, and with the average fading power set to 0 dB, sampled at 9600 samples/s.

4.4 Receiver Model

For these simulators, the single user and multiuser receiver [Car86], [Gib96] models, Figs. 4.9 and 4.10, respectively, turn out to be very simple. Somewhat similar transmitter and receiver constructions as used in this Thesis are presented in [Cav97]. The received total complex-valued signal, consisting now of the transmissions from all the users and some AWGN, is despread by multiplying it with the desired user's spreading code. Here it is assumed that the spreading codes are known and precisely synchronized. The despread signal is integrated over the bit duration to yield an estimate of the accumulated signal energy from the desired user. This is also the signal that is fed to the controller as input in the multiuser simulators. In the single user simulators, the input to the controller is the despread signal which is only decimated to yield a sampling rate equal to the bit rate. For clarity, the decimator is here shown within Fig. 4.9, even though in the simulator it resides within the controller block. The integrated signal is then BPSK demodulated. The COSSAP BPSK block also makes the bit decisions based on the Euclidean distances from the received complex signal samples to the constellation points. In the bit-error-rate (BER) calculation, the received signal is compared with the actual transmitted data.

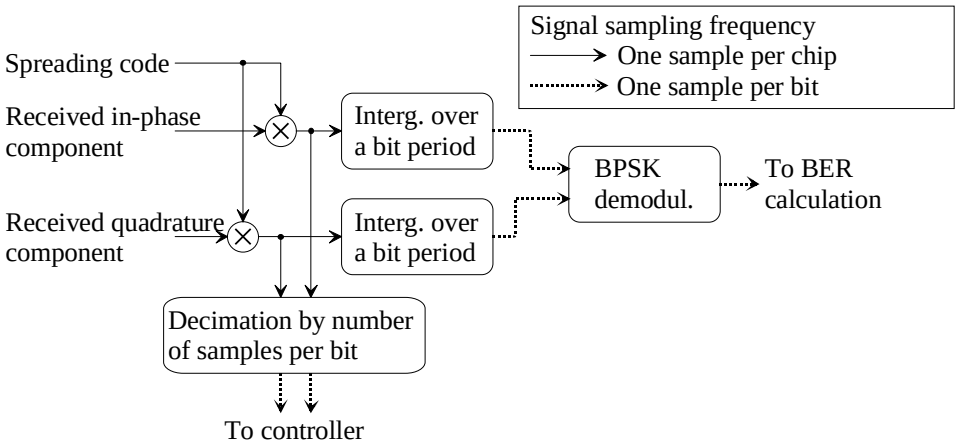

Fig. 4.9. Singleuser simulator receiver block diagram. In the simulator, the decimator resides within the controller but is shown here for the clarity.

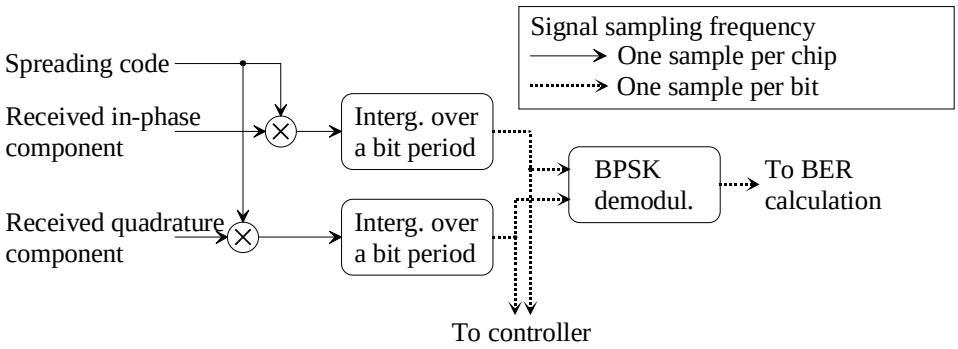

Fig. 4.10. Multiuser simulator receiver block diagram.

4.5 Power Controller Model

Increasing the capacity of a DS/CDMA system by improving the uplink power control system [Cha96], [Qua92] functionality is the motivation of the work presented in this Thesis, although predictive filtering in general is a powerful tool for variety of applications. It has been widely studied in the literature that the user capacity of a CDMA network is crucially dependent on the effectiveness of the power control system [Gil91], [Vit93b], [Ari], [Lee97], [Ada96]. This is because the system capacity is interference limited, and it is thus of great importance that all the mobile users are received at the base station at an equal constant power level. Also, the transmitter power of each mobile is to be kept as low as possible to reduce interference and save batteries. A closed power control loop is illustrated in Fig. 4.11.

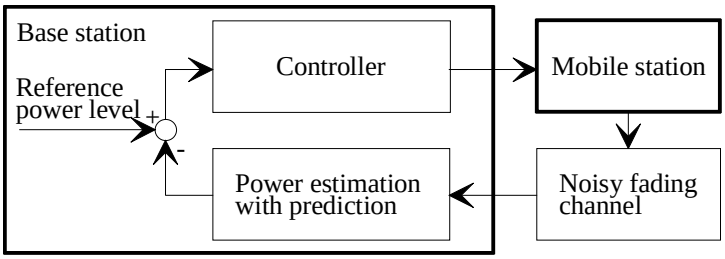

Fig. 4.11. A closed power control loop in a CDMA system.

A general reference to adaptive feedback, i.e., closed loop, control is [Åst87], and signal and interferences statistics for CDMA systems with closed loop power control are discussed in [Ari]. A CDMA system employs transmitter power control on both uplink [Qua92], [Cha96] and downlink [Qua92], [Lee95] direction. Only uplink power control functions are considered in this Thesis. In the downlink, it is generally possible to synchronize the transmissions and thus have better cross correlation properties between the CDMA codes at the mobile receiver. In the uplink this synchronization is not possible, or at least it is very difficult to realize.

4.5.1 The Qualcomm System Downlink Power Control

The uplink power control in the Qualcomm CDMA system [Qua92] includes both closed and open power control loops. The functioning of the open loop is based on the measurements made by the mobile station itself of the downlink channel, and therefore the measurement results are available for quick application. The open loop power control is used in situations where it is desirable to quickly reduce the transmitter power, as is the case, for example, when the mobile moves around a corner and a LOS path suddenly becomes available. This reduces unnecessary interference that would be caused otherwise. On the other hand, as the measurements are done from the downlink channel, and as the frequency separation between uplink and downlink channels, 45 MHz, exceeds the coherence bandwidth, the Rayleigh fadings are independent in the two channels, and thus the open loop power control cannot be used to fight the Rayleigh fading. The open loop control is also allowed to increase the transmitter power but the rate of increase is generally limited to the rate that the closed loop power control is able to compensate to avoid unnecessary interference in the case that the open loop decision had been wrong. The closed loop power control is based on the measurements done by the base station of the uplink channel. The base station sends power control commands to the mobile stations according to measured SNR, and the mobile station adjusts its transmitter power combining both open loop decisions and closed loop commands.

The open loop power control operation tries to maintain the power level received from all the mobile station on a constant nominal level and has dynamic range of about 85 dB or more. The closed loop power control response time is obviously slower than that of the open loop, but as the measurements are done in the uplink channel itself, the measurements show the actual Rayleigh fading in the channel and thus the closed loop power control is used to fight the Rayleigh fading. It is well understandable that in the this kind of closed loop control, latency minimization is of great importance as the channel should have remained essentially unchanged during the latency for the control to be effective. In the Qualcomm CDMA system, the power control commands are sent every 12 bits, i.e, every 1.25 ms, and the effect of each closed loop power control command to the mobile transmitter power is approximately ±0.5 dB.

4.5.2 Power Control in the Simulator

Power controller model block diagrams for single user and multiuser simulators are shown in Figs. 4.12 and 4.13, respectively. The input to the controller in the multiuser simulators is a signal which is already despread and integrated over the bit duration in the receiver. It is to be noted that the integration in the receiver readily removes much of the noise present in the received signal. The effect of this phenomenon is discussed in conjunction with the simulation result analysis.

The control is based on the estimated received signal power level originated from the mobile being controlled. The aim of the power control is to maintain the desired received power level irrespective of the fading and interference. It is assumed that the power control and data modulations of the received signal can be completely removed in order to obtain a predictable radio channel estimate which is then scaled by the number of chips per bit. It is assumed that in a real case, error correction coding [Qua92], [Vit95], [Gib96] and other means of improving BER would be used, and the system could provide low enough BER so that the phase error would be infrequent enough not to affect the controller performance too much. Here, as no error correcting coding is employed, i.e., the system produces so called raw BERs, there would be too many errors in the received data in order to do the data removal according to the actual received data, and thus ideal data modulation removal is assumed, and also transmitter power level setting is always known by the base station. The prediction is independently applied to the in-phase and quadrature components of this estimate. After prediction, the transmitter power level information is restored by multiplying the predicted chip components with the corresponding transmitter power level setting. Signal power estimate is calculated by computing the sum of squared in-phase and quadrature components, the power estimate is integrated over the control period in bits, and scaled by the number of bits in a control period. This presents the predictive estimate $\hat{P}_r$ (4.11) of the received average signal power originating from the particular user's mobile transmitter. The scalings are performed in order to be able to set the desired signal threshold level to unity, i.e., to 0 dB.

$$\hat{P}_r(n_c) = \frac{1}{M}\sum_{m=1}^{M}\left[c(n)\sum_{k=1}^{K} h(k)\frac{x_i(n-k)}{c(n-k)} + c(n)\sum_{k=1}^{K} h(k)\frac{x_q(n-k)}{c(n-k)} \right]^2, \qquad (4.11)$$

where n is the bit time index,
n_c the control command time index, sampled at the same time with every Mth n,

M the number of bits per control interval,
$c(n)$ the transmitter power level setting,
K the number of FIR coefficients,
$h(k)$ the coefficients of the predictive finite impulse response filter, and
x_i and x_q the in-phase and quadrature components of the controller input,
respectively, from which the power control and data modulations have been removed. The reference controllers are exactly identical with the corresponding predictive controllers, except that the predictors are omitted.

Finally, the power control bit to be sent to the mobile transmitter is generated using a threshold function, so that if the input to the thresholder is larger than 1 a control bit "1" is output to reduce the transmitter power, and correspondingly if the input to the thresholder is less than 1 a control bit "0" is output to command for increase in the mobile transmitter power level. The power controller setpoint is thus 0 dB. Possible power control bit transmission errors are not accounted for in the simulator.

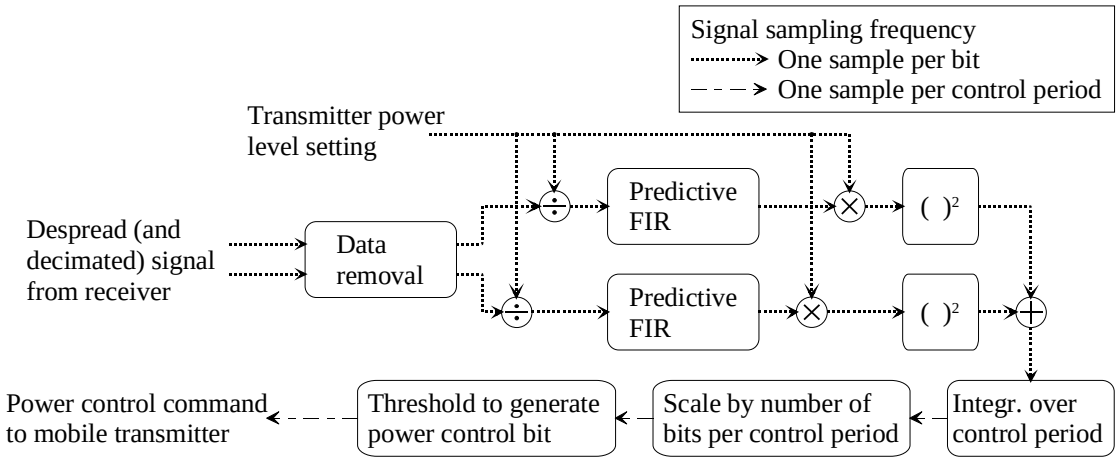

Fig. 4.12. Block diagram of the predictive singleuser power controller. Prediction is done in components at bit rate. In blocks with two input and two output signals, the processing is done independently to the upper and lower input signals. In the actual simulator, decimation of the input is done in the controller block.

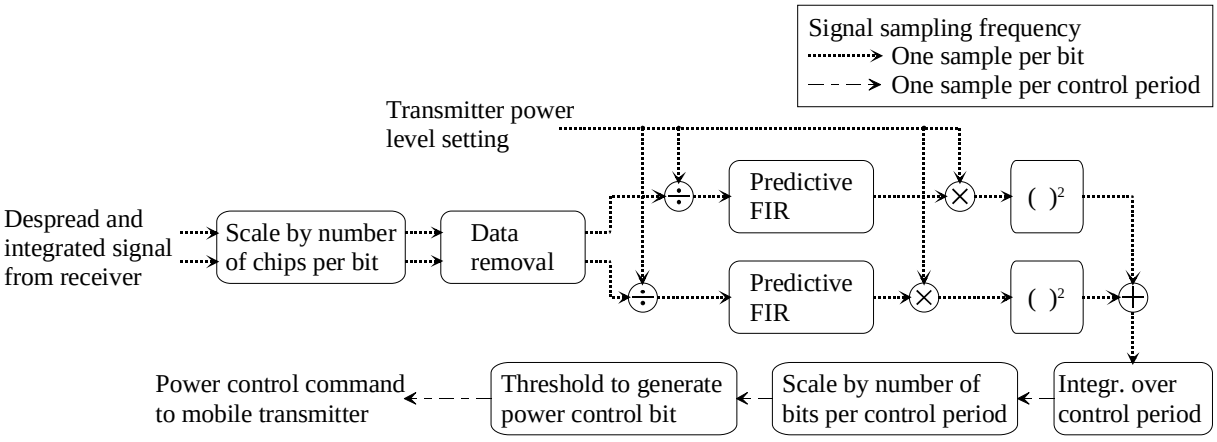

Fig. 4.13. Block diagram of the predictive multiuser power controller. Prediction is done in components at bit rate. In blocks with two input and two output signals, the processing is done independently to the upper and lower input signals.

For the control equations, please cf. [P3], [P5], and Chapter 8 Errata of *the Publications*.

5. Neural Networks in Mobile Power Control

As the radio channel statistics are constantly changing, and its parameters may be difficult to measure, neural networks may offer solutions to the received power level estimation problem, as well to a variety of other mobile communications system problems. Neural networks (NN) are attractive mostly because of their widely used abilities to learn the signal statistics, or other possible dependencies within the input data, if the network is properly constructed. This learning can be designed to be done either off-line with known input data, or on-line, i.e., the neural network can be made adaptive. A real-time adaptive neural network is naturally a computationally heavy solution but its advantages are also obvious.

Neural networks [Fre91], [Gao95] are capable of learning relations between input data and desired output data. In the context of this Thesis, neural networks could be used either in the actual prediction, or to estimate signal properties. In the former case, the input data to the network is a received power level history, and the output is the predicted power level. In the latter case, the same input is associated, for example, with the mobile speed, or with the length of the near-optimum polynomial predictor. In any case, the network has to be trained with either a known training set of input and output data covering the whole range of possible channel conditions, or with a suitable channel model. Also, as the polynomial prediction has been shown to be effective for power prediction, a representative set of polynomials could also be employed in the training. In operation, online adaptation can also be used regardless of whether the NN was also trained off-line or not.

5.1 Introduction to Neural Networks

One example of a possible NN topology [Fre91] is shown in Fig. 5.1. No processing is done in the input layer but the inputs are only distributed to the inputs of the computing elements in the next layer, which may be either a hidden layer, or the output layer. A possible hidden layer, or output layer, computing element, i.e., a neuron, is illustrated in Fig. 5.2. The neuron computes a weighted sum s of all its inputs x_i, and applies an activation function f to the sum. Result is then either a network output, or a hidden layer neuron output which is distributed to all the neurons in the next layer. Letting O denote an output of a neuron, it is given by

$$O = f\left(\sum_{i=1}^{M} w_i x_i\right). \tag{5.1}$$

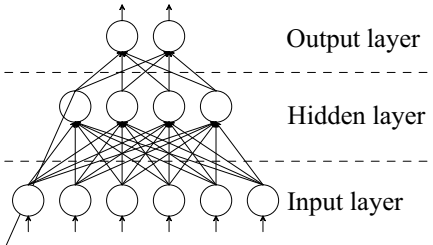

Fig. 5.1. A neural network with K=6 inputs and L=2 outputs.

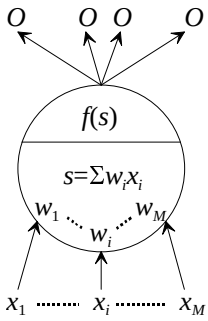

Fig. 5.2. A hidden layer or an output layer computing element with inputs x_i, weights w_i, an activation function f, and output O. In the first hidden layer M=K.

The activation function *f* may be, for example, a linear function, or a sigmoid function [Fre91]. Activation function is used to control the behavior of the outputs and intermediate results of the network to improve learning and to achieve desired outputs. The network in Fig. 5.1 is taught [Fre91], for example, by presenting a training input vector to the network inputs and calculating the outputs. The outputs are compared to the known desired outputs, and the errors are propagated down the network in the fractions according to the weights in each computing element. The weights are then updated with the backward propagated errors so that if the same input is presented to the network again, the output is closer to the desired output as before the training took place. This training approach is called error backpropagation [Fre91]. Training may also be continued online if desired. The network topology can either be selected by trial-and-error method, or an algorithmic optimization method may be used [Gao96], [Gao97a], [Gao97c]. As the intention of this text is to give the reader an idea of the possibilities of the NNs, let us not go now any deeper into NN training methods, or to topology optimization.

Generally, the NN topology has been found by trial and error methods, or by reducing the size of the NN until performance degradation is seen. The Gao brothers have successfully applied a criteria of predictive minimum description length (PMDL) [Ris84] to NN structure optimization [Gao96], [Gao97b], [Gao97c]. Their NN work concerning mobile power control is short described in the next section.

As nonlinear systems, NNs do not posses frequency responses in traditional sense. Even so, it is very insightful for a NN designer to estimate the properties of the networks trained, or under training. This also aids the designer in applicability considerations. In [Var97], input dependent frequency response estimates are obtained for a NN originally designed for Rayleigh fading prediction. Responses are estimated for sinusoidal [Nee90] and WGN input signals, and also time domain behaviors for step and triangular signals are observed. Similarities of the frequency response estimates from different input reflect good generalization capabilities of the NN.

5.2 Examples of Neural Networks in Mobile Power Control

In [Gao96], [Gao97c] a hybrid neural network based predictor, Fig. 5.3, is constructed for Rayleigh fading prediction. With online adaptation, the NN structure in Fig. 5.3, exhibits 3 to 5 dB better SNR gains than those obtained using H-N predictors but naturally the adaptive NN structure is computationally severely more expensive than the H-N predictor solutions. In [Gao96], [Gao97c] structures of both NNs, functional link NN, and multilayer perceptron, Fig. 5.3, are optimized using the PMDL principle. The functional link NN is essentially an adaptive FIR fed from a tapped delay line. Output of the functional link NN, Fig. 5.3, in turn feeds the tapped delay line input of the multilayer perceptron.

In [Gao97a] a Modified Elman Neural Network (MENN) based DS/CDMA closed loop power control system is presented. The MENN is shown in Fig. 5.4. This network type has the advantage of having a context layer. In the context layer, no actual processing is done but the nodes act as inner memory units storing the “context” in which the network is currently operating. Due to the internal context nodes and adaptive connection weights *w*, the structure is advantageous in identifying dynamic systems without knowledge on their exact order [Gao97a]. Also, a multiple model control system is sketched that consists of several system model identified off-line [Gao97a]. Switching between the models can be done, for example,

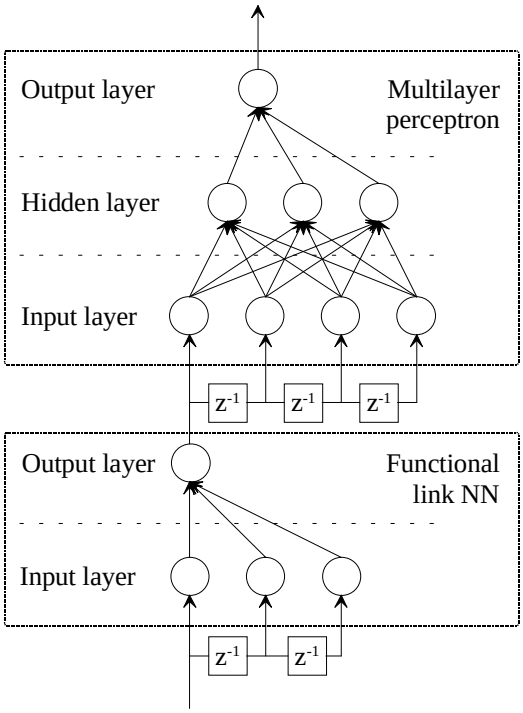

Fig. 5.3. A hybrid NN-based predictor structure (of an arbitrary size, for example only). Adopted from [Gao97c].

based on the mobile speed estimates. The system also includes a gain control subsystem which is necessary for obtaining quick power control responses when abrupt environmental changes occur, say when a mobile suddenly appears from behind a building creating a greatly improved radio propagation channel with a new LOS path between the mobile and the base station. In [Gao97a], MENN was able to reduce the deep fading to allow for successful communications also during some fades. The power control system presented in [Gao97a] is actually parametrized for deep fade reduction, and as such is thus not exactly suited for obtaining constant, and minimum acceptable, received power levels at the base station but the structure itself has great potential for the power control applications.

Two other interesting concepts are using optimal neuro-fuzzy predictors [Gao97b], and a temporal difference method-based prediction [Sut88], [Gao98] in mobile power control systems. In [Gao97b], structure of the neuro-fuzzy predictor is also optimized using the PMDL principle [Ris84]. The temporal difference-method based predictor [Gao98] is also based on MENN network structure, Fig. 5.4, while in contrast with the common direct signal value prediction, the actual function is designed for predicting the probability of deep fade incidents several steps ahead [Gao98]. The basis of the temporal difference method is to consider the difference between two successive predictor outputs as the prediction error [Sut88], [Gao98].

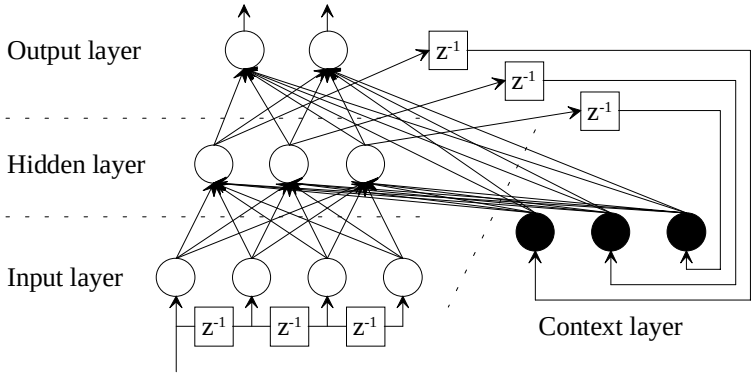

Fig. 5.4. Basic structure of a MENN of the size, selected for example only, K=4 inputs from a tapped delay line, L=2 outputs, three hidden layer and C=3 context layer neurons. Adopted from [Gao97a].

Possibilities of applying NNs to power signal prediction are numerous. NNs can be used to do the actual prediction, either direct power prediction, or prediction in components. They can be applied to radio channel modeling [Ibn97], or to adaptive channel equalization [Kec94]. In [Miy93] NN systems has been suggested for CDMA MUD. Furthermore, they could be used as signal derivative detectors, or to directly output the momentary predictor parameters. These application possibilities make NNs an interesting research topic in the field of power control

systems. One could even think of a pure neural network power controller that would directly generate the power control command to be sent to the mobile unit [Gao97a].

6. Conclusions and Discussions

In the beginning, this research concentrated on the possibilities of predicting Rayleigh fading [P1], [P2] with the mobile speeds were within urban speed range 5 km/h, …, 50 km/h, as in all the cases presented in *the Publications*. It was clearly seen that a Rayleigh fading signal, typically encountered in mobile communications, is very well predictable by the means of, for example, Heinonen-Neuvo polynomial predictors. In [P1] and [P2] H-N polynomial predictor performances are evaluated, and predictor selection criteria are given for two different Rayleigh fading models. It is also found that mainly due to the differing frequency distribution, more attention should be paid on the method for generating Rayleigh fading in mobile communications simulations than what is generally considered. Though, in the polynomial prediction study, these differences have only marginal effects. These results, stating the predictability of the Rayleigh fading, set forward the work to find out the effects of prediction in an actual closed loop power controller. In [P3], obvious results of applying lowpass predictors in a closed control loop whose actions are dictated by the excess noise power are very clearly shown. Results in [P3] apply to the case where only a single user can exist at any time within a given carrier frequency band, and the power controller input is the total received signal after despreading. In this case, the excess noise power reduction is of crucial importance for the closed control loop operation, and the need for filtering is illustratively shown. In [P4], an actual multiuser simulator is presented, and the results achieved by applying H-N predictors are given. The results indicate that marginal transmitter power savings and a little improved power control functionality may be achieved by applying H-N predictors. In [P5], results of applying both H-N polynomial predictors and optimum power estimators by A. Huang are presented for singleuser, 5- and 10-user, and AWGN multiuser interference model simulations, with the same main conclusions as in [P4].

The simulator construction work was naturally found to be full of compromises. In a way, it would have been of more practical interest to create a simulator with more realistically implemented radio channel and base station receiver models. The channel model could have been a complete multipath channel model with different fading distributions available, and the base station receiver could have consisted of an actual RAKE receiver, or some MUD schemes could have been applied. This would have made the work more interesting reading for practical radio engineers. From the signal processing point of view, these additions would have obscured the effects of predictive filtering to a very large extend. Even in the multiuser simulator presented here, the multiuser interference makes it somewhat more difficult to be able to clearly see and analyze the effects of individual system component improvements. Therefore, the research direction with very simple, yet scientifically justifiable, system models was adopted.

The simulated power control system was found to be very restrictive by itself, not leaving much room for improvements, i.e., the power control period is fairly long and fixed, and the power control step size and the overall power control system dynamics are naturally also limited. Anyway, the final conclusion is that a closed power control loop can be fine tuned with application of proper predictive filtering, which enhances the noise content of the received power level measurement data, and possibly slightly adjusts power control timing.

7. Summary of the Publications

P1 J. M. A. Tanskanen, A. Huang, T. I. Laakso, and S. J. Ovaska, "Polynomial prediction of noise shaping Rayleigh fading," in *Proc. 1995 Finnish Signal Processing Symposium*, Espoo, Finland, June 1995, pp. 26–29.

In [P1], predictivity of delayed and noisy Rayleigh fading signals with Heinonen-Neuvo polynomial predictors of several lengths and degrees is presented in the sense of achievable SNR gains. Rayleigh fading signal generation from WGN by noise shaping, and the applied predictors, are reviewed in the paper. Two prediction schemes for complex-valued signals are presented and an appropriate complex signal SNR definition is developed. The Rayleigh fading process parameters are derived partially from a CDMA communications system point of view, and the prediction is found to be a potential tool for received fading power level estimation in CDMA power control systems. The results are shortly compared with those employing prediction of Rayleigh fading generated by Jakes' fader. Also, the prediction of low frequency parts of the fading signals with regard to utilizing 'slow' fading information is considered, i.e., the signal used as the reference in SNR calculations can be band-limited. Anyway, the main emphasis in the paper is on the total fading signal prediction.

The main results of the paper are the polynomial predictor performance evaluation and H-N length and degree selection criteria for Rayleigh fading signals used at urban mobile speeds.

P2 J. M. A. Tanskanen, A. Huang, T. I. Laakso, and S. J. Ovaska, "Prediction of received signal power in CDMA cellular systems," in *Proc. 45th IEEE Vehicular Technology Conference*, Chicago, IL, July 1995, pp. 922–926.

In [P2], the predictivity of delayed and noisy Rayleigh fading signals with Heinonen-Neuvo polynomial predictors of several lengths and degrees is presented in the sense of achievable SNR gains. Jakes' Rayleigh fader and the applied predictors are reviewed in the paper. As compared to [P1], [P2] addresses the prediction of low frequency parts of the fading signals, whereas the emphasis of [P1] is in the complete signal prediction. [P2] thus emphasizes prediction of the frequency components of the Rayleigh fading received power level that is actually relevant to the CDMA power control function. For this, an appropriate complex signal SNR employing lowpass filtered reference signals is developed with special attention is paid to the reference signal generation. The applied H-N predictors and the complex-valued signal prediction schemes are reviewed.

The main results of the paper are the polynomial predictor performance evaluation and length and degree selection criteria for Rayleigh fading signals used. The differences between the noise shaping Rayleigh fader [P1] and the Jakes' fader [P2] affecting the prediction are analyzed in the introductory part of this Thesis.

P3 J. M. A. Tanskanen, J. Mattila, M. Hall, T. O. Korhonen, and S. J. Ovaska, "Predictive closed loop transmitter power control," in *Proc. 1996 IEEE Nordic Signal Processing Symposium*, Espoo, Finland, Sept. 1996, pp. 5-8.

In [P3], a single user CDMA closed loop power control simulator is constructed and H-N predictive control is compared with the corresponding non-filtered reference control. The system parameters are derived from Qualcomm CDMA system parameters with some modifications to speedup and simplify simulations. In the simulator, the input to the controller is the total unprocessed complex-valued received baseband signal. The results clearly demonstrate the effect of excess noise to the operation of the closed power control loop, with the main emphasis on the noise reduction capabilities of the filter used within the closed power control loop. The prediction mechanism of the H-N predictors is present but negligible with regard to the results shown.

In [P3], the selected total closed power control loop delay, 1 chip duration, is too short to be reality. This delay as a propagation delay would mean that the cell radius would be approximately only 122 m. Still, part of the delay consist of signal processing delays.

The main result is that this kind of closed loop power control, and thus also the data transmission, fails completely under too noisy conditions unless filtering is applied. The results illustratively show the definitive deed for filtering within the closed control loop based on the total received power estimation.

P4 J. M. A. Tanskanen, J. Mattila, M. Hall, T. Korhonen, and S. J. Ovaska "Predictive closed loop power control for mobile CDMA systems," in *Proc. 47th IEEE Vehicular Technology Conference*, Phoenix, Arizona, USA, May 1997, pp. 934-938.

In [P4], complete multiuser CDMA closed loop power control simulators are constructed with 5 or 10 users, one of which is the user under observation. The users are connected to a single base station, and interfere with each others. Also, a WGN multiuser interference model is simulated. In this simulator, the input to the controller is the complex-valued received signal after despreading and integration over the bit duration. This is the main difference with the controller employed in [P3]. As the result of the integration, noise power at the controller input has already been reduced, and the predictive function of the applied H-N lowpass predictors is more pronounced. The multiuser interference is clearly apparent in the control action results shown in the paper. It is shown, that the predictive controller is capable of commanding to reduce transmitter power earlier than the non-predictive controller. BER comparisons between the predictive and non-predictive controllers give no consistent results as the mobile speed and the number of users is varied. Though, as the BERs given in the paper, are raw BERs, i.e., e.g., no error correction coding is applied, the BER difference to one direction or to the other may not have any effect on the BER performance of an actual communications system. The predictive control results in consistent reduction in transmitter power consumption, though the achieved savings are very low, actually marginal, and statistically not very meaningful. However, the control objective, minimizing the variance of the received power level is consistently a little better achieved with the predictive controller than with the non-predictive reference controller. The WGN interference model results agree with the actual multiuser interference results in most of the cases.

The main result is that the closed power control loop can be fine tuned by application of proper predictive filtering, and H-N prediction is seen to be able to slightly adjust control timing.

P5 J. M. A. Tanskanen, A. Huang, and I. O. Hartimo "Predictive power estimators in CDMA closed loop power control," in *Proc. 48th IEEE Vehicular Technology Conference*, Ottawa, Ontario, Canada, May 1998, in press.

In [P5] two optimum predictor design methods based on the Wiener model are presented by A. Huang, and they are applied in single user, 5-user, 10-user, and AWGN interuser interference model closed power control loop simulators. Thus [P5] also offers a quick look at the actual multiuser simulator vs. the commonly used AWGN interuser interference model, as does [P4], too. Also, H-N polynomial predictors are employed as well as non-predictive power measurement based systems. The latter of which is used as the reference case. The simulation results are given in the form of achieved BERs, mobile transmitter power savings, and received power level variance reductions. The reduction of the received power level variance, or the variance of the user's channel output power, is the actual control variable whose quality is the main motivation behind the whole research work presented since the CDMA communications system capacity is greatly dependent on the power control system's capability of providing for equal and constant power levels at the base station receivers from all individual mobile users.

The single user results very clearly show the need for (predictive) filtering in this type of power controllers, as also concluded in [P3]. The multiuser simulation results show that even though the simulated power control system is inherently very restrictive, it is possible to fine tune the closed power control loop by application of proper predictors.

8. Errata of the Publications

In [P1]: The sum of two independent shaped Gaussian noise processes is guaranteed to be Rayleigh distributed.

should read: The absolute value of the sum of two independent shaped Gaussian noise processes with equal statistics is guaranteed to be Rayleigh distributed.

In [P2]:
$$SNR_{out} = \frac{\sum_n \left[\left(f\left(x_c(n+1)^2 + x_s(n+1)^2 \right) \right)^2 \right]}{\sum_n \left[\hat{y}(n) - \left(f\left(x_c(n+1)^2 + x_s(n+1)^2 \right) \right)^2 \right]} \quad (6)$$

should read
$$SNR_{out} = \frac{\sum_n \left[\left(f\left(x_c(n+1)^2 + x_s(n+1)^2 \right) \right)^2 \right]}{\sum_n \left[\left(\hat{y}(n) - f\left(x_c(n+1)^2 + x_s(n+1)^2 \right) \right)^2 \right]} \quad (6)$$

Also in [P2]:
$$y_c(n_c) = \frac{1}{C} \sum_{n=1}^{C} p(n)^2 \sum_{k=1}^{K} h(k) \cdot \left[\left(\frac{x_i(n-k+1)}{p(n-k+1)} \right)^2 + \left(\frac{x_i(n-k+1)}{p(n-k+1)} \right)^2 \right] \quad (5)$$

should read
$$y_c(n_c) = \frac{1}{C} \sum_{n=1}^{C} p(n)^2 \sum_{k=1}^{K} h(k) \cdot \left[\left(\frac{x_i(n-k+1)}{p(n-k+1)} \right)^2 + \left(\frac{x_q(n-k+1)}{p(n-k+1)} \right)^2 \right] \quad (5)$$

Also in [P2]:
$$y_c(n_c) = p_c(n_c)^2 \sum_{k=1}^{K} \left\{ h(k) \frac{1}{C} \sum_{m=1}^{C} \left[\left(\frac{x_i(n_c' - m + 1)}{p(n_c' - m + 1)} \right)^2 + \left(\frac{x_i(n_c' - m + 1)}{p(n_c' - m + 1)} \right)^2 \right] \Bigg|_{n_c' = n_c - Ck + C} \right\} \quad (7)$$

should read
$$y_c(n_c) = p_c(n_c)^2 \sum_{k=1}^{K} \left\{ h(k) \frac{1}{C} \sum_{m=1}^{C} \left[\left(\frac{x_i(n_c' - m + 1)}{p(n_c' - m + 1)} \right)^2 + \left(\frac{x_q(n_c' - m + 1)}{p(n_c' - m + 1)} \right)^2 \right] \Bigg|_{n_c' = n_c - Ck + C} \right\} \quad (7)$$

In [P4]: the chip frequency 1.2244 MHz

should read: the chip frequency 1.2288 MHz

Also in [P4]:
$$\hat{p}_{rec,c} = \frac{1}{M} \sum_{m=1}^{M} \left[p_{trans}(n) \sum_{k=1}^{K} h(k) \frac{x_i(n-k)}{p_{trans}(n-k)} + p_{trans}(n) \sum_{k=1}^{K} h(k) \frac{x_q(n-k)}{p_{trans}(n-k)} \right]^2 \quad (3)$$

should read
$$\hat{p}_{rec,c} = \frac{1}{M} \sum_{m=1}^{M} \left[\left(p_{trans}(n) \sum_{k=1}^{K} h(k) \frac{x_i(n-k)}{p_{trans}(n-k)} \right)^2 + \left(p_{trans}(n) \sum_{k=1}^{K} h(k) \frac{x_q(n-k)}{p_{trans}(n-k)} \right)^2 \right] \quad (3)$$

In [P5]: computationally every efficient.

should read: computationally very efficient.

9. References[†]

[Ada96] F. Adachi, "Theoretical analysis of DS-CDMA reverse link capacity with SIR-based transmit power control," *IEICE Trans. Fundamentals*, vol. E79-A, pp. 2028–2034, Dec. 1996.

[Ari93] S. Ariyavisitakul and L. F. Chang, "Signal and interference statistics of a CDMA system with feedback power control," *IEEE Trans. Commun.*, vol. 41, pp. 1626–1634, Nov. 1993.

[Ari94] S. Ariyavisitakul, "Signal and interference statistics of a CDMA system with feedback power control - Part II," *IEEE Trans. Commun.*, vol. 42, pp. 597–605, Feb./Mar./Apr. 1994.

[Bai94] A. Baier, U.-C. Fiebig, W. Granzow, W. Koch, P. Teder, and J. Thielecke, "Design study for a CDMA-based third-generation mobile radio system," *IEEE J. Selected Areas Commun.*, vol. 12, pp. 733–743, May 1994.

[Ban96] Y. J. Bang and S. W. Kim, "A new spreading scheme for convolutional coded CDMA communication in a Rayleigh-fading channel," *IEEE Trans. Commun.*, vol. 44, pp. 1537–1542, Nov. 1996.

[Cal88] G. Calhoun, *Digital Cellular Radio*. Norwood, MA, USA: Artech House, Inc., 1988.

[Cam91] T. G. Campbell and Y. Neuvo, "Predictive FIR filters with low computational complexity," *IEEE Trans. Circuits and Systems*, vol. 38, pp. 1067–1071, Sept. 1991.

[Cam96] R. Cameron and B. Woerner, "Performance analysis of CDMA with imperfect power control," *IEEE Trans. Commun.*, vol. 44, pp. 777–781, July 1996.

[Car86] A. B. Carlson, *Communication Systems, An Introduction to Signals and Noise in Electrical Communications*. New York, NY, USA: McGraw-Hill Book Company, 1986.

[Cav97] A. Cavallini, F. Gianetti, M. Luise, and R. Regiannini, "Chip-level differential encoding/detection of spread-spectrum signals for CDMA radio transmission over fading channels," *IEEE Trans. Commun.*, vol. 45, pp. 456–463, Apr. 1997.

[Cha94] N. L. B. Chan, "Multipath propagation effects on a CDMA cellular system," *IEEE Trans. Vehicular Tech.*, vol. 43, pp. 848–855, Nov. 1994.

[Cha96] C.-J. Chang, J.-H. Lee, and F.-C. Ren, "Design of power control mechanisms with PCM realization for the uplink of DS-CDMA cellular mobile radio system," *IEEE Trans. Vehicular Tech.*, vol. 45, pp. 522–530, Aug. 1996.

[Che97] K. Cheun, "Performance of direct-sequence spread-spectrum RAKE receivers with random spreading sequences," *IEEE Trans. Commun.*, vol. 45, pp. 1130–1143, Sept. 1997.

[Den93] P. Dent, G. E. Bottomley, and T. Croft, "Jakes fading model revisited," *Electronics Letters*, vol. 29, pp. 1162–1163, June 1993.

[†] Note on the nomenclature: In the case of several publications from an author on a given year being referenced all at once, references are jointly denoted by omitting the letter following the year. Similarly, all the publications listed from a given author are jointly referenced by omitting also the publication year.

[Eur93] European Telecommunications Standards Institute, *European Digital Cellular Telecommunication System (Phase 2); Radio Transmission and Reception, GSM 05.05, vers. 4.6.0*. Sophia Antipolis Cedex, France, July 1993.

[Fan95] J. Fang and L. E. Atlas, "Quadratic detectors for energy estimation," *IEEE Trans. Signal Processing*, vol. 43, pp. 2582–2594, Nov. 1995.

[Fre91] A. Freeman and D. M. Skapura, *Neural Networks: Algorithms, Applications, and Programming Techniques*. New York, NY, USA: Addison-Wesley Publishing Company, Inc., 1991.

[Gan72] M. J. Gans, "A power-spectral theory of propagation in the mobile-radio environment," *IEEE Trans. Vehicular Tech.*, vol. 21, pp. 27–38, Feb. 1972.

[Gao96] X. M. Gao, J. M. A. Tanskanen, and S. J. Ovaska, "Comparison of linear and neural network-based power prediction schemes for mobile DS/CDMA systems," in *Proc. 1996 Vehicular Technology Conference*, Apr. 1996, Atlanta, GE, USA, pp. 61-65.

[Gao97a] X. M. Gao, X. Z. Gao, J. M. A. Tanskanen, and S. J. Ovaska, "Power control for mobile DS/CDMA systems using a modified Elman neural network controller," in *Proc. 47th IEEE Vehicular Technology Conference*, Phoenix, AZ, USA, May 1997, pp. 750–754.

[Gao97b] X. M. Gao, X. Z. Gao, and S. J. Ovaska, "Power prediction using an optimal neuro-fuzzy predictor," in *Proc. IEEE Instrumentation and Measurement Technology Conference*, Ottawa, Canada, May 1997, pp. 1225–1230.

[Gao97c] X. M. Gao, X. Z. Gao, J. M. A. Tanskanen, and S. J. Ovaska, "Power prediction in mobile communication system using an optimal neural-network structure," *IEEE Trans. Neural Networks*, vol. 8, pp. 1446–1455, Nov. 1997.

[Gao98] X. Z. Gao and S. J. Ovaska, "A temporal difference method-based prediction scheme applied to fading power signals," accepted for publication in *Proc. 1998 IEEE International Conference on Neural Networks*, Anchorage, AK, USA, May 1998.

[Gej92] R. R. Gejji, "Forward-link-power control in CDMA cellular systems," *IEEE Trans. Vehicular Tech.*, vol. 41, pp. 532–536, Nov. 1992.

[Gib96] J. D. Gibson (ed.), *The Mobile Communications Handbook*. Boca Raton, FL, USA: CRC Press, Inc., and IEEE Press, 1996.

[Gil91] K. S. Gilhousen, I. M. Jacobs, R. Padovani, A. J. Viterbi, L. A. Weaver, Jr., and C. E. Wheatly III, "On the capacity of a cellular CDMA system," *IEEE Trans. Vehicular Tech.*, vol. 40, pp. 303–312, May 1991.

[Gra93] S. A. Grandhi, R. Vijayan, D. J. Goodman, and J. Zander, "Centralized power control in cellular radio systems," *IEEE Trans. Vehicular Tech.*, vol. 42, pp. 466–468, Nov. 1993.

[Gra94] S. A. Grandhi, R. Vijayan, and D. J. Goodman, "Distributed power control in cellular radio systems," *IEEE Trans. Commun.*, vol. 42, pp. 226–228, Feb./Mar./Apr. 1994.

[Har95] T. Harju and T. I. Laakso, "Polynomial predictors for complex-valued vector signals," *Electronics Letters*, vol. 31, pp. 1650–1652, Sept. 1995.

[Has79] H. Hasemi, “Simulation of the urban radio propagation channel,” *IEEE Trans. Vehicular Tech.*, vol. 28, pp. 213–225, Aug. 1979.

[Has93] H. Hasemi, “The indoor radio propagation channel,” *Proc. IEEE*, vol. 81, pp. 943–968, July 1993.

[Hei88] P. Heinonen and Y. Neuvo, “FIR-median hybrid filters with predictive FIR substructures,” *IEEE Trans. Acoustics, Speech, and Signal Processing*, vol. 36, pp. 892–899, June 1988.

[Hua95a] A. Huang, T. I. Laakso, S. J. Ovaska, and I. Hartimo, “Predictive power estimation of complex-valued signals,” in *Proc. 38th Midwest Symp. Circuits and Systems*, Rio de Janeiro, Brazil, Aug. 1995, pp. 953–956.

[Hua95b] A. Huang, T. I. Laakso, S. J. Ovaska, and I. O. Hartimo, “On schemes for power prediction of complex-valued signals,” in *Proc. 1995 Finnish Signal Processing Symposium*, Espoo, Finland, June 1995, pp. 55–58.

[Hua96a] A. Huang and T. I. Laakso, “Power estimation approaches for complex-valued signals based on Hammerstein model and Wiener model,” in *Proc. Nordic Signal Processing Symposium*, Sept. 1996, Espoo, Finland, pp. 191–194.

[Hua96b] A. Huang, T. I. Laakso, S. J. Ovaska, and I. Hartimo “Optimal linear power estimator for slowly-varying complex-valued signals,” in *Proc. The Third International Conference on Signal Processing*, Oct. 1996, Beijing, China, pp. 76–79.

[Hua96c] A. Huang and T. I. Laakso, “Optimal design and adaptive implementation of power estimation using Hammerstein model,” in *Proc. IEEE 39th Midwest Symposium on Circuits and Systems*, Aug. 1996, Ames, Iowa, USA, pp. 18–21.

[Hua97] A. Huang, *Efficient Methods for Power Estimation—Optimization and Implementation*. Licentiate Thesis, Helsinki University of Technology, Espoo, Finland, May 1997.

[Hua98] A. Huang, J. M. A. Tanskanen, and I. O. Hartimo, “Design and Application of Efficient Optimum Power Estimator Based on Wiener Model for Complex-Valued Signals,” accepted for publication in *Proc. of 1998 IEEE International Symposium on Circuits and Systems*, May 1998, Monterey, CA, USA.

[Ibn97] M. Ibnkahla, J. Sombrin, F. Castanie, and N. J. Bershad, “Neural networks for modeling nonlinear memoryless communication channels,” *IEEE Trans. Commun.*, vol. 45, pp. 768–771, July 1997.

[IEE88] IEEE Vehicular Technology Society Committee on Radio Propagation, N. H. Shepherd (Chairman), “Coverage prediction for mobile radio systems operating in the 800/900 MHz frequency range,” *IEEE Trans. Vehicular Tech.*, vol. 37, pp. 3–72, Feb. 1988.

[Jak74] W. C. Jakes (ed.), *Microwave Mobile Communications.* New York, NY, USA: John Wiley & Sons, Inc., 1974.

[JaH94] L. M. A. Jalloul and J. M. Holtzman, “Multipath fading effects on wide-band DS/CDMA signals: analysis, simulation, and measurements,” *IEEE Trans. Vehicular Tech.*, vol. 43, pp. 801–807, Aug. 1994.

[JaM94] A. Jalali and P. Mermelstein, “Effects of diversity, power control, and bandwidth on the capacity of microcellular CDMA systems,” *IEEE J. Sel. Areas Commun.*, vol. 12, pp. 952–961, June. 1994.

[Kal85] N. Kalouptsides, G. Carayannis, D. Manolakis, and E. Koukoutsis, "Efficient recursive in order least squares FIR filtering and prediction," *IEEE Trans. Acoustics, Speech, and Signal Processing*, vol. 33, pp. 1175–1187, Oct. 1985.

[Kec94] G. Kechriotis, E. Zervas, and E. S. Manolakos, "Using recurrent neural networks for adaptive communication channel equalization," *IEEE Trans. Neural Networks*, vol. 5, pp. 267–278, Mar. 1994.

[Kim93] K. I. Kim, "CDMA cellular engineering issues," *IEEE Trans. Vehicular Tech.*, vol. 42, pp. 345–350, Aug. 1993.

[Kim97] J. Y. Kim and J. H. Lee, "Effect of imperfect power control on acquisition performance in a DS/CDMA system," *Electronics Letters*, vol. 32, pp. 1255–1256, July 1996.

[Kud92] E. Kudoh and T. Matsumoto, "Effects of power control error on the system user capacity of DS/CDMA cellular mobile radios," *IEICE Trans. Commun.*, vol. E75-B, pp. 524–529, June 1992.

[Kud93] E. Kudoh, "On the capacity of DS/CDMA cellular mobile radios under imperfect transmitter power control," *IEICE Trans. Commun.*, vol. E76-B, pp. 886–893, Aug. 1993.

[Laa93] T. I. Laakso and S. Ovaska, "Optimal polynomial predictors with application specific fixed prefilters," in *Proc. IEEE Int. Symp. Circuits and Systems*, Chicago, IL, May 1993, pp. 351–354.

[Lee86] W. C. Y. Lee, *Mobile Communications Design Fundamentals*. Indianapolis, IN, USA: Sams, 1986.

[Lee91] W. C. Y. Lee, "Overview of Cellular CDMA," *IEEE Trans. Vehicular Tech.*, vol. 40, pp. 291–302, May 1991.

[Lee95] T.-H. Lee, J.-C. Lin, and Y. T. Su, "Downlink power control algorithms for cellular radio systems," *IEEE Trans. Vehicular Tech.*, vol. 44, pp. 89–94, Feb. 1995.

[Lee97] J. Lee, R. Tafazolli, and B. G. Evans, "Erlang capacity of OC-CDMA with imperfect power control," *Electronics Letters*, vol. 33, pp. 295–261, Feb. 1997.

[Li95] V. O. K. Li and X. Qui, "Personal communication systems (PCS)," *Proc. of IEEE*, vol. 83, pp. 1210–1243, Sept. 1995.

[Lin92] J.-P. M. G. Linnartz, R. Hekmat, and R.-J. Venema, "Near-far effects in land mobile random access networks with narrow-band Rayleigh fading channels," *IEEE Trans. Vehicular Tech.*, vol. 41, pp. 77–90, Feb. 1992.

[Lin97] X. D. Lin and K. H. Chang, "Optimal PC sequence design for quasisynchronous CDMA communication systems," *IEEE Trans. Commun.*, vol. 45, pp. 221–226, Feb. 1997.

[Loo91] C. Loo and N. Secord, "Computer models for fading channels with applications to digital transmission," *IEEE Trans. Vehicular Tech.*, vol. 40, pp. 700–707, Nov. 1991.

[Mag94] D. T. Magill, F. D. Natali, and G. P. Edwards, "Spread-spectrum technology for commercial applications," *Proc. IEEE*, vol. 82, pp. 572–584, Apr. 1994.

[Mil92] L. B. Milstein, T. S. Rappaport, and R. Barghouti, “Performance evaluation for cellular CDMA,” *IEEE J. Selected Areas Commun.*, vol. 10, pp. 680–689, May 1992.

[Miy93] T. Miyajima, T. Hasegawa, and M. Haneishi, “On the multiuser detection using a neural network in code-division multiple-access communications,” *IEICE Trans. Commun.*, vol. E76-B, pp. 961–968, Aug. 1993.

[Nee90] J. Neejärvi and Y. Neuvo, “Sinusoidal and pulse responses of FIR-median hybrid filters,” *IEEE Trans. Circuits and Systems*, vol. 37, pp. 1552–1556, Dec. 1990.

[Orf90] S. J. Orfanidis, *Optimum Signal Processing*: *An Introduction* (2nd ed.). New York, NY, USA: McGraw-Hill Book Company, 1990.

[Ova91a] S. J. Ovaska, “FIR prediction using Newton’s backward interpolation algorithm with soothed successive differences,” *IEEE Trans. Instrumentation and Measurement*, vol. 40, pp. 811–815, Oct. 1991.

[Ova91b] S. J. Ovaska, “Newton-type predictors – A signal processing oriented viewpoint,” *Signal Processing*, vol. 25, pp. 251–257, Nov. 1991.

[Ova92] S. J. Ovaska and O. Vainio, “Recursive linear smoothed Newton predictors for polynomial extrapolation,” *IEEE Trans. Instrumentation and Measurement*, vol. 41, pp. 510–516, Aug. 1992.

[Par87] W. Parks and C. S. Burrus, *Digital Filter Design*. New York, NY, USA: John Wiley Sons, Inc., 1987.

[Par92] D. Parsons, *The Mobile Radio Propagation Channel*. London, England: Pentech Press limited, 1992.

[Pic82] B. Picinbono, “Quadratic filters,” in *Proc. Int. Conf. Acoustics, Speech, and Signal Processing*, Paris, France, May 1982, pp. 298–301.

[Pic91] R. L. Pickholtz, L. B. Milstein, and D. L. Schilling, “Spread Spectrum for Mobile Communications,” *IEEE Trans. Vehicular Tech.*, vol. 40, pp. 313–322, May 1991.

[Pov96] G. J. R. Povey, P. M. Grant, and R. D. Pringle, “A decision-directed spread-spectrum RAKE receiver for fast-fading mobile channels,” *IEEE Trans. Vehicular Tech.*, vol. 45, pp. 491–502, Aug. 1996.

[Pra92] R. Prasad, A. Kegel, and M. G. Jansen, “Effect of imperfect power control on cellular code division multiple access system,” *Electronics Letters*, vol. 28, pp. 849–848, Apr. 1992.

[Pri58] R. Price and P. E. Green, “A communication technique for multipath channels,” *Proc. of IRE*, pp. 555–570, Mar. 1958.

[Pri96] F. D. Priscoli and F. Sestini, “Effects of imperfect power control and user mobility on a CDMA cellular network,” *IEEE J. Sel. Areas Commun.*, vol. 14, pp. 1809–1817, Dec. 1996.

[Pro92] J. G. Proakis and D. G. Manolakis, *Digital Signal Processing: Principles, Algorithms, and Applications*. New York, NY, USA: Macmillan Publishing Company, 1992.

[Qua92] QUALCOMM Incorporation, *An Overview of the Application of Code Division Multiple Access (CDMA) to Digital Cellular Systems and Personal Cellular Networks*. (Document no. EX60-10010), 1992.

[Ran92] J. P. Ranta, S. J. Ovaska, and T. I. Laakso, “Adaptive polynomial predictor for feedback velocity prefiltering in elevator control,” in *Proc. Int. Conf. Signal Processing Applications and Technology*, Cambridge, MA, Nov. 1992, pp. 583–592.

[Ris84] J. Rissanen, “Universal coding, information, prediction, and estimation using predictive MDL principle,” *IEEE Trans. Information Theory*, vol. 30, pp. 629–636, July 1984.

[Sch90] D. L. Schilling, R. L. Pickholtz, and L. B. Milstein, “Spread spectrum goes commercial,” *IEEE Spectrum*, pp. 40–45, Aug. 1990.

[Sha97] M. Shafi, A. Hashimoto, M. Umehira, S. Ogose, and T. Murase, “Wireless communications in the twenty-first century: a perspective,” *Proc. of IEEE*, vol. 85, pp. 1622–1638, Oct. 1997.

[Sic92] G. Sicuranza, “Quadratic filters for signal processing,” *Proc. of IEEE*, vol. 80, pp. 1263–1285, Aug. 1992.

[Sim85] M. K. Simon, J. K. Omura, R. A. Scholtz, and B. K. Levitt, *Spread Spectrum Communications, Vol. 1, Vol. 2*. Rockville, MD, USA: Computer Science Press, 1985.

[Sim93] F. Simpsom and J. M. Holtzman, “Direct sequence CDMA power control, interleaving, and coding,” *IEEE J. Sel. Areas Commun.*, vol. 11, pp. 1085–1095, Sept. 1993.

[Str96] E. G. Ström, S. Parkvall, S. L. Miller, and B. E. Ottersten, “Propagation delay estimation in asynchronous direct-sequence code-division multiple access systems,” *IEEE Trans. Commun.*, vol. 44, pp. 84–93, Jan. 1996

[Sut88] R. S. Sutton, “Learning to predict by the methods of temporal differences,” *Machine Learning*, vol. 3, pp. 9–44, 1988.

[The92] C. W. Therrien, *Discrete Random Signals and Statistical Signal Processing*. London, UK: Prentice-Hall International, Inc., 1992.

[Ton94] O. K. Tonguz and M. M. Wang, “Cellular CDMA networks impaired by Rayleigh fading: System performance with power control,” *IEEE Trans. Vehicular Tech.*, vol. 43, pp. 515–527, Aug. 1994.

[Vaj95] I. Vajda, “Code sequences for frequency-hopping multiple-access systems,” *IEEE Trans. Commun.*, vol. 43, pp. 2553–2554, Oct. 1995.

[Val97] R. A. Valenzuela, O. Landron, and D. L. Jacobs, “Estimating local mean signal strength of indoor multipath propagation,” *IEEE Trans. Vehicular Tech.*, vol. 46, pp. 203–212, Feb. 1997.

[Wan93] M. M. Wang and O. K. Tonguz, “Forward link power control for cellular CDMA networks,” *Electronics Letters*, vol. 29, pp. 1195–1197, June 1993.

[Var97] B. Varone, J. M. A. Tanskanen, and S. J. Ovaska, “Response analysis of a feed-forward neural network,” in *Proc. 1997 International Conference on Acoustics, Speech, and Signal Processing*, Munich, Germany, Apr. 1997, pp. 3309-3312.

[Vit93a] A. J. Viterbi, A. M. Viterbi, and E. Zehavi, “Performance of power-controlled wideband terrestrial digital communication,” *IEEE Trans. Commun.*, vol. 41, pp. 559–569, Apr. 1993.

[Vit93b] A. M. Viterbi and A. J. Viterbi, “Erlang capacity of a power controlled CDMA system,” *IEEE J. Selected Areas Commun.*, vol. 11, pp. 892–900, Aug. 1993.

[Vit94a] A. J. Viterbi, A. M. Viterbi, and E. Zehavi, “Other-cell interference in cellular power-controlled CDMA,” *IEEE Trans. Commun.*, vol. 42, pp. 1501–1504, Feb./Mar./Apr. 1994.

[Vit94b] A. J. Viterbi, “The evolution of digital wireless technology from space exploration to personal communication services,” *IEEE Trans. Vehicular Tech.*, vol. 43, pp. 638–644, Aug. 1994.

[Vit95] A. J. Viterbi, *CDMA Principles of Spread Spectrum Communication*. Reading, MA, USA: Addison-Wesley Publishing Company, 1995.

[Zan92] J. Zander, “Performance of optimum transfer power control in cellular radio systems,” *IEEE Trans. Vehicular Tech.*, vol. 41, pp. 57–62, Feb. 1992.

[Åst87] K. J. Åström, “Adaptive feedback control,” *Proc. of IEEE*, vol. 75, pp. 185–217, Feb. 1987.

PUBLICATION P1

J. M. A. Tanskanen, A. Huang, T. I. Laakso, and S. J. Ovaska
"**Polynomial prediction of noise shaping Rayleigh fading**"
in
Proc. 1995 Finnish Signal Processing Symposium
Espoo, Finland, June 1995, pp. 26–29.

PUBLICATION P2

J. M. A. Tanskanen, A. Huang, T. I. Laakso, and S. J. Ovaska
"**Prediction of received signal power in CDMA cellular systems**"
in
Proc. 45th IEEE Vehicular Technology Conference
Chicago, IL, July 1995, pp. 922–926.

PUBLICATION P3

J. M. A. Tanskanen, J. Mattila, M. Hall, T. O. Korhonen, and S. J. Ovaska
"**Predictive closed loop transmitter power control**"
in
Proc. 1996 IEEE Nordic Signal Processing Symposium
Espoo, Finland, Sept. 1996, pp. 5-8.

PUBLICATION P4

J. M. A. Tanskanen, J. Mattila, M. Hall, T. Korhonen, and S. J. Ovaska
"**Predictive closed loop power control for mobile CDMA systems**"
in
Proc. 47th IEEE Vehicular Technology Conference
Phoenix, Arizona, USA, May 1997, pp. 934-938.

PUBLICATION P5

J. M. A. Tanskanen, A. Huang, and I. O. Hartimo
"**Predictive power estimators in CDMA closed loop power control**"
in
Proc. 48th IEEE Vehicular Technology Conference
Ottawa, Ontario, Canada, May 1998, in press.